Role of the Endothelin System in Normal Development

Farideh Bayan

Department of Pathology

McGill University

Montreal, Quebec, Canada

A thesis submitted to the Faculty of Graduate Studies and Research

In partial fulfillment of the requirements for the degree of

Master of Science

F. Bayan

August 1995

ISBN 0-612-12158-5

In the name of God

Abstract

Endothelins are a family of 21 amino acid peptides that act on G protein-coupled heptahelical receptors. The original member of the endothelin family, endothelin-1 (ET-1), was identified as a potent vasopressor derived from vascular endothelial cells. Three known mammalian endothelins, ET-1, ET-2, and ET-3, are each encoded by separate genes and expressed in a variety of vascular and nonvascular tissues. Two subtypes of endothelin receptors have been identified and termed endothelin-A and endothelin-B receptors (ET-A and ET-B). In the first part of this study, the ET-A gene was disrupted in mouse embryonic stem cells to generate mice deficient in ET-A. These ET-A homozygous mice died of respiratory failure at birth and showed morphological abnormalities of the pharyngeal-arch-derived craniofacial tissues and organs, indicating the importance of ET-A in the normal development of the neural crest-derived tissues.

In the second part of this study, we investigated a targeted disruption of the mouse ET-B gene that results in aganglionic megacolon associated with coat color spotting, resembling a hereditary syndrome of mice, humans and other mammalian species (Waardenburg syndrome) . These findings indicate an essential role for the ET-B in the development of two neural crest-derived cell lineages, myenteric ganglion neurons and epidermal melanocytes.

In the third part of this study, we demonstrated that a targeted disruption of the mouse endothelin-3 ligand (ET-3) gene produces a similar recessive phenotype of megacolon and coat color spotting. These findings indicate that interaction of ET-3 with the ET-B is essential in the development of neural crest-derived cell lineages.

ET-1 is converted from biologically inactive big ET-1 to biologically active ET-1 by the action of endothelin converting enzymes (ECEs). Two types of endothelin converting enzymes (ECE-1 and ECE-2) have been recently identified. In the last part of this study, we investigated the expression of ECE-1 in human tissues using immunohistochemistry and in situ hybridization, and compared it to those of ET-1 and big ET-1. Histological examination of specimens revealed that the pattern of ECE-1-ir was parallel to ET-1 and big ET-1. In situ hybridization showed expression of the mRNA in similar sites to those of immunostaining. These findings indicate ECE-1 is widely expressed in human tissues and its level of expression may differ under various pathological states.

Résumé

Les endothélins sont une famille de 21 acides amines peptides qui agissent sur les recepteurs heptahelicals. Le membre original de la famille d'endothélin-1 (ET-1), a été identifié comme un vasopresseur dérivé des cellules vasculaires endothéliales. Trois endothélins mammiferes connus, ET-1, ET-2, et ET-3, sont tous encodés par des genes séparés et presents dans une variété de tissues vasculaires et non-vasculaires. Deux sous-types de recepteurs endothélins ont été identifiés comme récepteurs endothélin-A et endothélin-B (ET-A et ET-B). Dans la première partie de cette étude, le gene ET-A a été interrompu dans le cellule souche embryonique de souris afin de génerer des souris déficientes en ET-A. Ces souris homozygotes ET-A sont mortes de défaillance respiratoire à la naissance et ont montré des anamalies morphologiques des tissus crano-faciaux et organes arc pharyngiens, indiquant l' importance de l' ET-A dans le développement normal des tissus cretes neurales.

Dans la seconde partie de cette recherche, nous avons étudié une interruption ciblée du gene ET-B de la souris, qui résulte en un mégacolon congénital associé à des taches de couleur de la fourrure, ressenblant à un syndrome héréditaire de la souris, de l'homme et d'autres espèces mammiferes (Syndrome Warrdenburge). Ces découvertes indiquent le role essentiel de l'ET-B dans le dévelopment de deux cretes neurals de cellules dérivées lineages ganglions mésentériques et les mélanocytes épidermaux.

Dans la troisième partie de cette étude, nous avons démontré qu'une interruption ciblée du gene endothélin-3 (ET-3) de la souris produit un phenotype récessif similaire du mégacolon et des taches sur la fourrure. Ces découvertes indiquent que l'interaction de l'ET-3 avec l'ET-B est essentielle dans le développement des tissus cretes neurals.

L'ET-1 est converti à partir du biologiquement inactif et large ET-1 au biologiquement actif ET-1 par l'action des enzymes convertisseurs endothélins (ECEs). Deux types d'enzymes convertisseurs (ECE-1 et ECE-2) ont été récemment identifiés. Dans la derniére partie de cette étude, nous avons examiné la présence de l'ECE-1 dans les tissus humains en utilisant l'immunohistochimie et l hybridation in situ, et l'avons comparé à ceux de l'ET-1 et du large ET-1. L'examen histologique des specimens a révélé que le patron de l'ECE-1-ir est parraléle au ET-1 et au large ET-1. L'hybridation in situ a démontré la présence du mRNA dans sites similaires de l'immuno coloration. Ces découvertes indiquent que l ECE-1 est largement présent dans les tissus humains et que son niveau de présence peut varier selon divers états pathologiques.

Acknowledgment

First of all, I must thank God for giving me health, strength and patience during my Master program.

I wish to express my gratitude to the following people who have participated each in their own way to the development and completion of this work.

I would like to thank my research director, Dr. A. Giaid, for giving me the opportunity to work on this research project, and for his skillful guidance and contribution throughout the course of this study, and a very precise review of this thesis.

I would also like to thank:

- Dr. E. Zorychta and Dr. W.P. Duguid for their understanding and kindness and providing me the opportunity to finish this project.
- Dr. K. Furukawa for her helpful discussions throughout the course of my work.
- Miss D. Saleh and Mrs. N. Chikhani for introducing me to laboratory techniques.
- My husband for his understanding and encouragement throughout my studies, my little boy Ali, and my parents for all of their kindness and support from so far away throughout my studies.

The partial financial assistance of Iranian Ministry of Health and Medical Education is appreciated.

Table of Contents

List Of Figures

List of Abbreviations

AVP: arginine vasopressin.

Ca^{2+}: calcium ion.

cDNA: complementary deoxyribonucleic acid.

CNS: central nervous system.

CSF: cerebrospinal fluid.

DNA: Deoxyribonucleic acid.

ES : embryonic stem.

ET-1: endothelin type 1.

ET-2: endothelin type 2.

ET-3: endothelin type 3.

ET-A: endothelin receptor type A.

ET-B: endothelin receptor type B.

ET-C: endothelin receptor type C.

G-protein: guanine nucleotide-binding protein.

GFR: glomerular filtration rate.

irET: immunoreactive endothelin.

M: mol per liter.

mRNA: messenger ribonucleic acid.

Na^+: sodium ion.

NEP: neutral endopeptidase

No: nitric oxide.

PBS: phosphate-buffered saline.

PCR: Polymerase chain reaction.

PGI_2: prostacycline.

RBF: renal blood flow.

RC-PCR: reverse transcription Polymerase chain reaction.

RNA: Ribonucleic acid.

SMC: smooth muscle cell.

SSC: standard sodium citrate.

TK: thymidine kinase.

VSMC: vascular smooth muscle cell.

$[Ca^{2+}]$: intracellular free calcium ion concentration.

μm: micrometer.

Chapter 1

Introduction

1.1 Discovery of endothelins

Key discoveries in the past two decades revealed that endothelial cells synthesize and release vasorelaxant (Moncada et al., 1976; Furchgott et al., 1980), and vasoconstrictor (De May et al., 1982; Rubanyi and Vonhoutte, 1986) substances. In 1982, a bioassay study led to the discovery of a peptidergic endothelium-derived contracting factor (EDCF) (Hickey et al., 1985). In 1987, a group of Dr. Masaki isolated, purified, sequenced and cloned this peptidergic EDCF, which they named endothelin (ET) (Yanagisawa et al., 1988).

1.2 Isotypes of endothelin

Analysis of human genomic sequences revealed the existence of three distinct genes for ET; these encode three distinct ET peptides (Clozel et al., 1989) and were named endothelin-1 (ET-1), ET-2 and ET-3. These three isomers present slightly different N-terminal amino acid sequences yet similar biological activities. ET-1 has been described as the most potent vasoconstrictive agent released by the endothelium (Schini et al., 1991).

There are three distinct ET-related genes in humans and other mammalian species. In the human, the ET-1, ET-2 and ET-3 genes have been mapped to chromosome 6

(Parker-Botelho et al., 1992; Inoue et al., 1989), chromosome 1 (Parker-Botelho et al., 1992; Inoue et al., 1989) and chromosome 20 (Inoue et al., 1989; Arinami et al., 1991). Thus, the genes encoding endothelin-related peptides are located on distinct human chromosomes.

1.3 Endothelin releasing cells

The formation and release of ET-1 has been characterized first in human (Yanagisawa et al., 1988), bovine, and porcine cultured endothelial cells (Emori et al., 1989). ET-1 is also produced by many types of cells, including neurons, epithelial cells, leukocytes, macrophages, cancer cell lines, among others. ET-1 production or release in endothelial and other cells is regulated by various vasoactive substances, growth factors, cytokines, and procoagulants among other factors (Yoshizumi et al., 1989; Schini et al., 1991). ET-3 has been shown to be released by neuronal and endothelial cells (EC) (Yamaji et al., 1990). Even though ET-2 has also been shown to be released mainly by EC, its presence (mRNA) in the kidney medulla may prove to be physiologically important.

1.4 Structure of endothelin peptides

The ET family consists of the three ET isoforms and four highly homologous cardiotoxic peptides. All family members contain 21 amino acid residues and show complete identity at ten positions, including all four cysteine residues (positions 1, 3, 11, and 15), as well as position 8 (aspartic acid), 10 (glutamic acid), 16 (histidine), 18 (aspartic acid), 20 (isoleucine), and 21 (tryptophan) (Arinami et al., 1991).

All three ET isoforms are synthesized as larger preproforms which are processed by dibasic amino acid endopeptidase activities to propeptides of 37 to 41 amino acids, the so called big ETs. The subsequent cleavage of these propeptides to the mature ETs is inefficient both in vitro and in vivo, because big ETs have been identified in plasma (Miyauchi et al., 1989) and in the media of the cultured cells (Parker-Botelho et al., 1992).

In the ETs, all four cysteine residues participate in disulfide bonding (Cys^1-Cys^{15}; Cys^3-Cys^{11}). It is now clear that the disulfide bonds present in the ETs are vital for high affinity binding to one of ET receptors (ET-A) but less important in recognition by another class of ET receptors (ET-B).

1.5 Mechanisms of endothelin biosynthesis

Primary translation product of the human ET-1 gene is a 212-amino acid prepropeptide (Bloch et al., 1989). Processing occurs in three stages: (a) dibasic amino acid endopeptidase(s) cleaves the precursor at Arg^{52}-Cys^{53} and at Arg^{92}-Ala^{93}, (b) carboxypeptidase(s) sequentially trims the Arg^{92} and Lys^{91} residues from the COOH

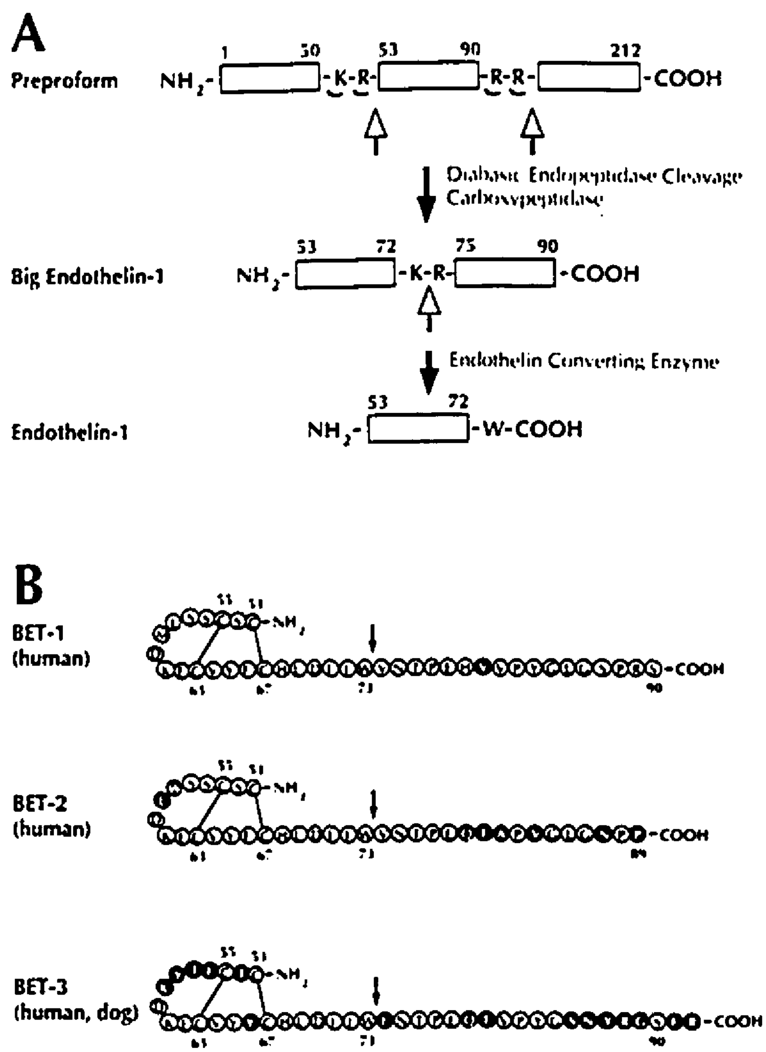

Figure 1.1. Posttranslational processing of prepro-ETs. A, 203-amino acid human prepro-ET-1 peptide is cleaved by dibasic amino acid endopeptidase action at two sites (arrows, top), followed by sequential carboxypeptidase activity (small curved arrows) to yield prepro-ET-1 (53 to 91), referred to as pro ET-1 or big ET-1 (middle).The COOH terminal portion of prepro-ET-1 contains the ET-1 like peptide. Big ET-1 is then cleaved by ECE to yield the final 21-amino acid product, ET-1.

Illustrations taken from Phillips et al., 1992.

terminus to produce pro-ET-1, more commonly known as big ET-1; (c) specific cleavage between Trp^{73}-Val^{74} by ECE yields ET-1.

The physiological importance of the conversion of big ET to ET was demonstrated by the observation that ET-1 was 140-fold more potent as a vasoconstrictor compared to the precursor peptide (Kimura et al., 1989), whereas the prepropeptide is devoid of any vasoconstrictor action. Molecular conversion of big ET-1 to mature ET-1, which is essential for the full expression of its biologic activity (Inoue et al., 1989), is dependent on putative endothelin converting enzymes (ECEs) (Figure 1.1).

1.6 Endothelin converting enzymes

Initially, the endothelin converting enzymes (ECEs) activity was suggested to be chymotrypsin-like enzymes (serin protease) (Mc Mahan et al., 1990). Products of chymotrypsin-treated analog of porcine big ET-1, big-ET (1-40 a.a.), produced in vitro and in vivo responses similarly to ET itself (Kimura et al., 1989). Using various experimental models, ECE was later associated to an aspartic protease (pepsin or cathepsin-like activity at pH<5.5) and a metalloprotease (Inoue et al., 1989). The ECE-like activity related to an aspartic protease was found in both cultured bovine and porcine aortic endothelial cells (Matsumura et al., 1991), bovine adrenal medulla (Yanagisawa et al., 1988), and rat lung (Sawamura et al., 1990). The metalloprotease type of enzymes presenting activity at pH 7.4 were later found in cultured bovine and porcine aortic endothelial cells (Sawamura et al., 1990), bovine and porcine vascular smooth muscle cells , in human and rat brain (Warner et al., 1992) as well as in whole blood. Therefore, there could be two and possibly more different types of ECE activity that convert big ET-1 to ET-1 in vascular EC (Hioki et al., 1991) or SMC (Matsumura et al., 1991); a membranous and a cytosolic one. The activity in the cytosolic fraction would be associated to a thiol-dependent soluble metalloprotease. Recent evidence strongly suggests that the physiologically relevant ECE is of the metalloendopeptidase type, hence a neutral endopeptidase (NEP 24.11). The activity of the phosphoramidon sensitive-ECE is also present in other systemic vasculatures or tissues (Hioki et al., 1991) as well as in the microcirculation (Matsumura et al., 1991). The specific conversion of big ET-1 into ET-1 was also demonstrated in the central nervous system and the urogenital tract; both the choroid plexus and kidney are rich in endopeptidase 24.11 (Lehoux et al., 1992).

The pathophysiological relevance of such an ECE-activity for the conversion of big ET-1 to its active ET-1 relies on two observations: first, it was shown that the pharmacologic effects of big ET-1 on systemic and regional hemodynamics (Bourne et al., 1992) can be abolished by phosphoramidon (D'Orleans et al., 1990). The conversion and biologic activation of big ET-1 to ET-1 was specific to a phosphoramidon-sensitive NEP because thiorphan, which is also an inhibitor of NEP, had much less effect on cardiovascular response to exogenous big ET-1 (Fukuroda et al., 1990). Moreover, partially purified ECE from bovine lung membrane was not affected by thiorphan, but inhibited by phosphoramidon (Mc Mahom et al., 1991). Secondly, phosphoramidon inhibited the release of ET-1 from EC (Knudact and Wilson, 1992). Interestingly, it was shown that treatment with phosphoramidon lowers blood pressure in spontaneously hypertensive rats (Ikegawa et al., 1990).

Determination of the intraluminal secretion and local levels of ET in vessel wall and tissues is helpful in providing evidence for ET turnover and its implication in local cell to cell interaction and on the regulation of vascular tone. In addition, conditions which affect ECE activity may be instrumental in the fluctuations of circulating levels of ET. Preliminary results (Naruse et al., 1991) suggest that the biosynthetic and/or degradation process of ET under pathologic conditions such as acute myocardial infarction, congestive heart failure, essential hypertension, vasospastic angina appears to be different from that observed under normal conditions.

1.7 Endothelin receptors

Shortly after the cloning and characterization of the three ET isoforms, it became obvious that saturable, high-affinity -binding sites for these peptides exist on cell membranes. It was presumed that, like other bioactive peptides, ETs produced their physiological effects through binding to these putative receptor sites. Many studies further suggested that the many diverse physiological and pharmacological effects of ETs could not be mediated by a single receptor subtype. Prior to the discovery of specific ET receptor antagonists, receptor

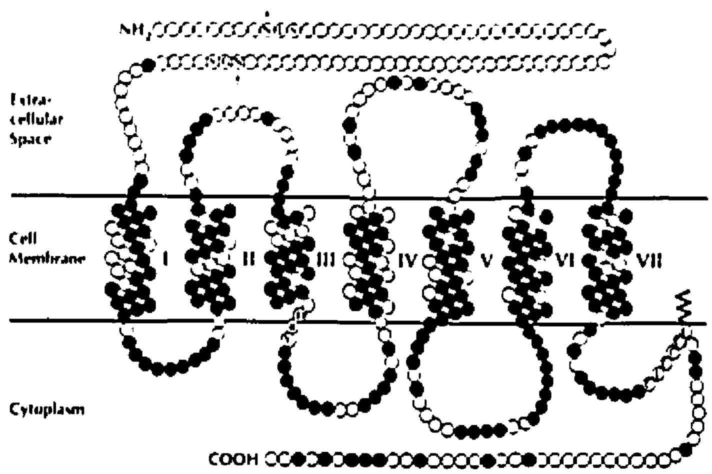

Figure 1.:2 Primary structure of the human ET-A receptor. The receptor is proposed to consist of an extracellular NH_2-terminal region, seven transmembrane helices separated by three extracellular and three cytoplasmic loops, and a cytoplasmic COOH-terminal region, residues that are conserved in the human ET-B receptor sequence. Also shown are two potential N-linked glycosylation sites in the NH_2-terminal region (arrows), the conserved sequence Asp-Arg-Tyr (D-R-Y) at the end of transmembrane helix III, which may be important in G-protein coupling, and the sequence Cys-Leu-Cys-Cys-Cys-Cys (C-L-C-C-C-C) in the COOH-terminal region believed to direct the myristylation of a cysteine, which may be important in stabilization of the extracellular ligand-binding site.

subtype classification were made on the basis of rank order potencies of either binding or function.

Two subtypes of endothelin receptors have been identified and named endothelin-A and endothelin-B receptors (ET-A and ET-B) (Arai et al., 1990; Sakomoto et al., 1993; Sakuria et al., 1990). There is evidence for the existence of a third receptor type (ET-C) (Karne et al., 1993). The cDNA encoding of this third receptor type is still unidentified. These receptors are also expressed in various target cells with a partially overlapping tissue distribution. In blood vessels, for example, vascular smooth muscle cells express ET-A or ET-B, both of which can mediate the direct vasoconstrictor action of endothelins. ET-A receptor exhibits different affinities for endothelin isopeptide ligands with a potency range order of ET-1≥ ET-2≥ ET-3 (Yanagisawa et al., 1994). ET-B receptor accepts all three isopeptides equally. Both receptors initiate several intracellular signal transduction events via heterometric G proteins, leading to a variety of biological actions. These include the activation of phospholipase Cβ, inhibition of adenyl cyclase, activation of plasma membrane Ca^{2+} channels, and activation of nonreceptor tyrosine kinases such as focal adhesion kinase P^{125FAK} (Rubanyi and Polokoff, 1994; Simonson and Herman, 1993; Zachary and Rozengurt et al., 1992).

As is typical for the members of the G-protein-coupled receptor superfamily, the genes for ET-A and ET-B are large, spanning 40 and 24 kb of DNA, respectively. The human ET-A gene is present on chromosome 4 and the ET-B gene is present on chromosome 13.

Recenuy a selective ET-A antagonist, BQ-123, has been shown to block the pressor response induced by exogenously administered ET-1 in the circulation of conscious rats (Ihara et al., 1992). However, this antagonist was not found to affect basal mean arterial pressure in the same animal species. Since ET-A receptors have in fact been partly localized on smooth muscle, ET-1 may interact with these receptors to induce vasoconstriction. It has been reported that BQ-123 competitively block the response of ET-1 in coronary blood vessels (Ihara et al., 1992). This suggests that ET acts directly on ET receptors in the coronary vasculature after which DHP calcium channels may then be indirectly activated by a mechanism associated to receptor-operated calcium channels.

1.8 Mechanisms of actions

Among the many biological actions of ETs observed so far, the vasoconstrictor property of ET-1 was the first to be recognized and most widely studied. Similarly, the signal transduction mechanisms triggered by binding of ET-1 to ET-A receptors in vascular smooth muscle are the most extensively analyzed and best understood so far.

1.8.1 Signal transduction pathway mediating short term changes in cell function

Endothelin-1-induced contractions of isolated blood vessels are more slowly developing, are maintained for a longer time, and are more resistant to agonist removal than are

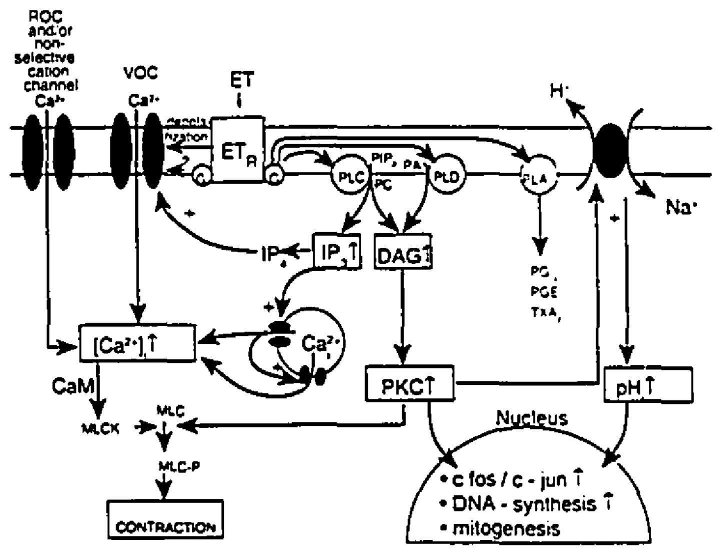

Figure 1.3 Signal transduction mechanisms involved in ET-1 induced short-term and long term modulation of cell function. CaM, calmodulin; ET_R, ET receptors; IP_4, 1,3,4,5-inositol tetrakisphosphate; MLCK, myosin light chain kinase; PIP_2, Phosphatidylinositol diphosphate; PA, phosphatidic acid; PC, phosphatidylcholine; PGE_2, prostaglandin E_2; PLA_2, phospholipase A_2; PLD, phospholipase D; ROC, receptor-operated calcium channel.

contractions evoked by most other vasoconstrictor agents. It is generally accepted that, in most vascular smooth muscle preparations, ET-1 interacts with a specific cell surface receptor, the ET-A type. In some vascular beds, ET-B subtype is also involved in smooth muscle contraction. Several receptor signal transduction mechanisms were suggested to be involved in ET-1-induced vascular contraction, and include (a) increase in cytosolic free calcium concentration ([ca^{2+}]) by facilitation of ca^{2+} influx and mobilization of intracellular ca^{2+}; (b) G-protein-mediated activation of phospholipase C (PLC), leading to phosphatidyl inositol hydrolysis and rapid formation of inositol monophosphate (IP) and sustained *sn*-1,2-diacylglycerol (DAG) accumulation; (c) activation of protein kinase C (PKC); (d) activation of phospholipase A_2 and D and arachidonic acid metabolism; and (e) changes in intracellular pH alkalinization via stimulation of Na^+-H^+ exchange (Rubanyi and Polokoff, 1994) (Figure 1.3).

1.8.2 Nuclear signal transduction mediating long-term effects on cell function

The finding that ET-1 is a mitogen for cultured vascular smooth muscle cells (Komuro et al., 1988), fibroblasts (Takuwa et al., 1989), adrenal zona glomerulosa cells (Simonson et al., 1989) suggested that, in addition to short-term signal transduction pathways mediating rapid endothelin-1-induced biological actions such as muscle contraction, ET-1 may regulate gene expression to evoke long-lasting cellular responses as well.

Indeed, ET-1 stimulated the expression of the immediated early response gene *c-fos* in VSMCs, 3T3 fibroblasts, and mesangial cell (Muldoon et al., 1989). ET-1 also stimulated the transcription of *c-myc* gene in VSMCs and V^{L30} gene transcription in fibroblasts (Simonson et al., 1990).

Although the signaling pathway(s) mediating the transcription of genes after ET-1 binds to its specific receptor on the plasma membrane are not known, elevation of $[ca^{2+}]$, activation of PKC, tyrosine, and threonine phosphorylation of mitogen-activation protein kinases, and stimulation of Na^{+}-H^{+} exchange, and consequent cytosolic alkalinization, were all proposed to play some role (Rubanyi and Polokoff, 1994) (Figure 1.3).

1.9 Actions of endothelin in various biological systems

1.9.1 Cardiovascular system

Intravenous infusion of ET-1 causes rapid and transient vasodilation, followed by a profound and long-lasting increase in blood pressure. The vasodilator effect was proposed to be due to activation of the vascular endothelium, leading to formation of PGI_2 (De Nucci et al., 1988) and endothelium-derived NO (Botting and Vane, 1990). ET-1 is the most potent endogenous substance known to induce contraction of isolated blood vessels. In general, these contractions are initiated by binding of ET isopeptides to ET-A receptor on vascular smooth muscle (Arai et al., 1990).

The direct cardiac actions of ETs induced positive inotropic (Baydon et al., 1989) and chronotropic effects (Karwatowska Prokopczuk and Wemmalm, 1990) as well as a prolongation of the action potential duration (Watanobe et al., 1989). ETs also affect heart function indirectly via profound coronary vasoconstriction. Studies with cultured myocytes suggest that ETs may be involved in cardiac hypertrophy as well.

1.9.2 Kidney

ET is secreted at several sites in the kidney, where it acts in a paracrine or autocrine fashion on ET receptors on target cells. Because of its biological actions (including vasoactive properties), ET probably contributes to the control of RBF, renal plasma flow, GFR, and sodium and water transport at different nephron sites. Systemic infusion of ET-1 increases renal vascular resistance (Tsuchiya et al., 1989) and markedly decreases RBF and GFR. (Badr et al., 1989).

1.9.3 Lung

ET-1 is a potent constrictor of smooth muscle in trachea and bronchus isolated from guinea pig, man and many other species (Ninomiya et al., 1992; Henry et al., 1990). Because of the three isopeptides, ET-1 proved to be the most potent constrictor of airway smooth muscle (Advenier et al., 1990), the response is probably mediated by the ET-A receptor subtype.

In the airway epithelium, ET-1 stimulates ciliary beat frequency in cultured canine tracheal epithelial cells by elevating [Ca^{2+}] (Tamaoki et al., 1991), suggesting that the peptide may play a role in modulating airway mucociliary transport function. ET-1 also inhibited methacholine and phenylephrine-stimulated ferret tracheal submucosal gland secretion of mucous and lysosomal enzymes and of active albumin transport across the epithelium (Yurdakos and Webber, 1991). Giaid et al have also shown that increased expression of ET-1 in pulmonary epithelial and endothelial cells may reflect a disease-specific activation of the cell types, which possibly contributes to the pathogenesis of cryptogenic fibrosing alveolitis (CFA) (Giaid et al., 1993a) and pulmonary hypertension (Giaid et al., 1993b)

1.9.4 Female reproductive system

ET-1, ET-2, and ET-3 cause contraction of rat (Borges et al., 1989), rabbits (Suzuki, 1990), guinea pig (Eglen et al., 1989), sheep (Yang and clark, 1992), and human uterus (Svane et al., 1993). ET-1 causes two types of contractions in rat uterus: phasic contractions, which can be inhibited by ca^{2+} channel antagonist, and tonic contractions, which are extracellular ca^{2+} concentration dependent but intensive to ca^{2+} channel antagonists (Kozaka et al., 1989). ET-1 contracts both nonpregnant and midpregnant uterus. The phasic, but not the tonic, contractions could be inhibited by ca^{2+} channel antagonists.

1.9.5 Male reproductive system

In leydig cells isolated from rat testis, ET-1 and to a lesser extent, ET-3 stimulate basal and human chorionic gonadotropin-induced testosterone production (Conte et al., 1993). Therefore, ET-1 may play a role in modulating steroid production in the testis via a paracrine mechanism.

1.9.6 Endocrine system

ETs interact with several endocrine systems and hormones, including the renin-angiotensin system, aldosteron, AVP, and arterial natriuretic peptide. These interactions exist at the level of both biosynthesis and biological actions (Rubanyi and Polokoff, 1994).

1.9.7 Central nervous system

Intracerebroventricular infusion of ET-1 in rats and rabbits increased plasma catecholamine, AVP, glucose, and adrenocorticotropic hormone levels and enhanced renal sympathetic nerve activity (Makino et al., 1990; Matsumura et al., 1991). vasopressinergic receptor antagonists, adrenergic receptor antagonists, and ganglionic blockade attenuated or completely abolished the pressor response (Kawano et al., 1989), suggesting that centrally administered ET-1 activates the sympathoadrenal and AVP systems, which mediate the central pressor response.

1.10 Presence of endothelin in body fluids

Significant quantities of ET-1-ir are detected in circulating plasma in several species, including humans (Parker-Botelho et al., 1992). The circulating plasma concentration of ET-1 are in the low picomolar range in healthy humans, which can be elevated 2-to 30-fold in various pathological conditions (Masaki et al., 1992).

In addition to the circulating peptide, irET has been detected in human urine. It was found that concentrations of ET were on average 6 fold higher in urine than in plasma. Similarly, ET is present in normal human CSF at levels that are significantly greater (approximately 7 fold) than in plasma (Rubanyi and Polokoff, 1994). ET has also been quantified in bronchial lavage fluid where the levels were elevated during the bronchospastic phase of an asthma attack and returned to basal level after recovery (Nomura et al., 1989).

Chapter 2

Role of the Endothelin-B Receptor Gene in Normal Development

2.1 Introduction

Development of the neural crest has been focus of intensive investigation. Neural crest cells arise from the dorsal neural tube shortly after its closure and migrate extensively through prescribed regions of the embryos, where they differentiate into most of the peripheral nervous system as well as the facial skeleton and pigment cells (Anderson et al., 1994, Bronner-Fraser et al., 1994). Along the embryonic axis, several distinct neural crest populations differ both in their migratory pathways and range of derivatives. A number of naturally occurring as well as targeted mutations in mice result in specific defects in various neural crest-derived cell lineages. Findings obtained by examining many mutant mice [i.e. mutation at the dominant spotting (W) and steel (Sl) loci (Jackson 1991), targeted disruption of the c-ret receptor tyrosine kinase (Pachnis et al., 1993; Schuchardt et al., 1994), knockout of the basic-helix-loop-helix (bHLH) transcription factor mammalian achaete-scute homolog 1 (Mash 1) (Guillemot et al., 1993)], point to important roles in neural crest development of receptor tyrosine kinases and their growth factor ligands, as well as lineage-specific transcription factors.

Hereditary defects in the development of epidermal melanocytes and myenteric ganglion neurons, two neural crest-derived cell lineages, often appear together. Such defects occur in mice (Lane et al., 1966; Lyon and Searle 1989), rats (Ikadai et al., 1979), horses (Mccabe et al, 1990) and humans (Shah et al., 1981). All of them manifest neurocristopathy (i.e. localized pigmentary disorder associated with aganglionic megacolon) (Liang et al., 1983). This strongly suggests that these two cell lineages share a common regulatory pathway in the crucial phases of their development from the neural crest.

Among the mouse mutations that produce this phenotypic combination, the piebald mutants have been characterized in most detail (Pavan and Tilghmon, 1994; Silvers, 1979). Homozygous s/s mice, which carry a mild mutation at this locus, manifest white spotting in about 20% of the coat and almost never manifest megacolon. In contrast, mice homozygous for a more severe mutant allele, s^1, are almost completely white and invariably manifest megacolon. These cells normally migrate dorsal to the somites and through the mesenchymal layer beneath the ectoderm, eventually entering the epiderms. The restriction of the pigment defect to skin melanocytes indicates that the coat color spotting is due to a disruption of the development of neural crest-derived melanocytes precursors, rather than to a defect in the ability to produce melanin.

The megacolon in s^l/s^l homozygotes is caused by the absence of enteric ganglia in the distal large intestine (Webster et al., 1973). The defect in s^l/s^l mice might be in any one or a combination of the stages involved in the normal development of these two neural crest-derived cell lineages. This includes their lineage determination, proliferation, migration along the unique paths, or local differentiation and survival in their final destination.

Here we show that a null mutation induced by targeted disruption of the mouse endothelin-B receptor (ET-B) gene results in a recessive phenotype of coat color spotting and aganglionic megacolon, closely resembling the phenotype manifested by mice homozygous for the piebald-lethal mutation. We also demonstrate that ET-B gene indeed allelic to the piebald locus, as indicated by a lack of complementation between these nulls and piebald mutations.

Note: This part of project was done in a collaborative work with the Howard Hughes Medical Institute and Department of Molecular Genetics in Dallas, Texas.

2.2 *Experimental procedures*

2.2.1 *Mutant mouse strains*

SSL/Lc s/s^1 and SSL/Lc s/s breeding pairs were obtained from The Jackson Laboratory. Homozygous s^1/s^1 mice were generated by crossing the s/s^1 mice.

2.2.2 *Targeted disruption of mouse ET-B gene*

To target the ET-B gene in mouse embryonic stem (ES) cells, a replacement vector was constructed by substituting a 4.2 kb segment of cloned mouse genomic DNA containing the ET-B exon 3 with a neomycin resistance (neo) cassette. In the next step of targeting this genes, herpes simplex virus thymidine kinase (TK) cassettes were added to the 3' end of the targeting vector for positive-negative selection (Ishibashi et al., 1993). A 129/Sv mouse ES cell line (Rosahi et al., 1993) was transfected with the linearized targeting vector, and the cells were selected for double resistance to G418 and FIAU (1-[2-deoxy-2-fluoro-ß-D-arabinofuranosyl}-5-iodo-uracil). 500 double-resistant colonies were screened of ET-B targeting gene by polymerase chain reaction (PCR), and ~ 20% of these clones were positive for targeted insertion of the cassette. Six of these PCR-positive ES clones were injected into blastocysts from C57BL/6J mice. Southern blot analysis confirmed that these ES cell clones of ET-B gene had a correctly targeted their allele.

2.2.3 Histology

Mice were perfusion fixed with formalin immediately after sacrifice, and tissues were dissected and further immersion fixed in formalin. After being embedded, the tissues were cut (5 microns). The slides were dried for 20 min. at 100°C and then dewaxed. The staining was carried out by immersing the slides in hematoxylin (5 mins), acid alcohol (99% alcohol and 1% hydrochloric acid 6 N) (5 secs) distilled water (5 mins), eosin (5 mins), 95% alcohol (5 secs) as a standard procedure of hematoxylin and eosin staining (Kafman, 1992a). Sections were then examined under bright-field microscopy .

2.2.4 Skeletal examination

For bone examination, the double staining method of C.Arrnot was used (Kaufman, 1992b). The tissues were fixed in 80% ethanol for 24 hrs and dehydrated in 96% ethanol for 24 hrs and then acetone for 3 days. Staining was carried out for 6 hrs using the following solution: 0.1% alizarin red S in 95% ethanol (1 ml), 0.3% alcian blue in 95% ethanol (1 ml) and 1% acid-alcohol (99 ml). The tissues were cleared with 96% ethanol for 1 hr, 1% aqueous KOH for 48 hrs and 50% glycerin in 1% aqueous KOH for 2 weeks. The tissues were then stored in 100% glycerin.

2.2.5 *In situ hybridization*

In situ hybridization was carried out by a modification of a method reported previously (Giaid et al., 1991). ET-B probes were labeled with ^{35}S-UTP using a commercial kit (Ambion Inc., Austin, TX). Frozen sections (10 μm thick) were mounted on poly-L-lysine coated slides and dried at 37°C overnight. The sections were rehydrated in PBS, permeabilized with proteinase K and then fixed in 4% paraformaldehyde. To reduce background noise, an acetylation step in triethanolamine and acetic anhydride was carried out followed by a solution of n-ethylmaleimide and iodoacetomide. Sections were hybridized at 42°C for 16 hours with the radiolabeled probes for ET-B. Unbound probe was removed by immersing sections in a solution containing RNAse A. Washes at 22-55°C in descending concentrations of sodium saline citrate was followed. Sections were then processed for autoradiography. Negative control experiments involved the use of sense probes and incubation of sections with the hybridization buffer in absence of the radiolabeled probe.

2.2.6 Radioligand binding assay

Kidney membrane fractions were prepared from freshly sacrificed mice as described previously (Bolger et al., 1990). Binding assay was carried out as described earlier (Bolger et al., 1990) with 10^{-11} M[^{125}I] endothelin-1 as tracer and using 30 μg of membrane protein per reaction. Nonspecific binding was determined in the presence of 10^{-7} M unlabeled endothelin-1 and was ~ 8% of total binding in the wild-type membranes. ET-B binding was determined by subtracting specific binding of [^{125}I] endothelin-1 in the presence of 10^{-7} M IRL1620 from that in the absence of the competitor.

2.3 Results

2.3.1 Morphology

Heterozygous F1 mice were phenotypically normal. F2 offspring were obtained by intercrossing F1 heterozygotes. A total of 93 F2 mice of ET-B on day 3 postpartum: 24, 49, and 20 mice were typed as ET-B$^-$/ET-B$^-$, ET-B$^-$/+, and +/+ animals were genotyped. These genotyping were compatible with Mendelian inheritance and indicated that homozygosity did not cause lethality in utero or shortly after birth.

The first obvious phenotype of the homozygous mice was extensive white spotting of the coat, which became apparent by days 3-4 (Figure 2.1 A). In the homozygous mice, the skin and coat were completely white in >90% of the body surface area, usually with small, well-demarcated pigmented area(s) in the head and hip regions. The normally pigmented areas were rarely symmetrical and occurred largely at random. The coat color within these pigmented areas was completely normal agouti or black, depending on the agouti background inherited. The eyes were dark in all cases. Most homozygous mice appeared otherwise healthy in the first few weeks after birth However, usually at 2-4 weeks of age, these mice became increasingly sick and emaciated. Their gain of weight retarded as compared with wild-type or heterozygous mice. Eventually, all homozygous died prematurely. The median and average life span of 30 randomly chosen homozygous mice were 27 and 25 days, respectively (range, 8-57 days).

An autopsy was performed on many homozygous mice, which were sacrificed at a time we estimated to have been 1-2 days before they would have died. We observed a gross distention of the intestine in all animals (Figure 2.1 C). In some cases, we observed a perforation of the distended intestine associated with severe peritonitis. Dissection of the entire gastrointestinal tract revealed that the distal portion of the colon was narrow and spastic and that the immediately proximal portion was markedly distended (Figure 2.1 D). In a majority of cases, the spastic segment spanned from the sigmoid colon to the distal rectum. However, the extent of the spastic segment varied; in some cases, it spanned only 2-3 mm in the most distal part of the rectum, while in two cases the entire colon was spastic, giving the appearance of microcolon. In all cases, however, the spastic segment extended to the most distal rectum. These gross anatomical features were consistent with the diagnosis of aganglionic megacolon. We did not detect any other gross anatomical abnormalities in the Homozygous ET-B mice.

Histological examination was consistent with the gross anatomical phenotype of the homozygotes. Figure 2.2 compared longitudinal sections of the colon from a wild-type and an homozygous ET-B mouse. The myenteric (Auerbach) ganglion neurons were clearly visible between the outer longitudinal and inner circular layers of smooth muscle cells along the entire length of the wild-type colon. These neurons were completely absent from the distal, spastic segment of the homozygous ET-B colon (Figure 2.2 A), but not from the proximal, distended portion (Figure 2.2 B). Agangliosis was histologically demonstrated in samples from all homozygous mice examined.

Microscopic examination of skin sections from the homozygotes confirmed an absence of melanin pigment in the coat hair and of melanocytes in the hair bulbs in the regions where the coat was white. The amount of hair pigment and the number of epidermal melanocytes seemed to be normal in the skin sections from the pigmented regions, reflecting the normal gross appearance of these regions. Sections of the eye from homozygous ET-B mice revealed a lack of melanin pigment in the choroidal layer of the retina (Figure 2.2 D). In contrast, the melanin content in the pigment epithelium appeared normal, consistent with the dark eyes of the homozygote mice. In the wild-type retina, we observed both layers of melanin pigment (Figure 2.2 E). These observations are consistent with the idea that the homozygous ET-B mice have defects in the development of neural crest-derived melanocytes (i.e., epidermal and choroidal melanocytes) but not in the neuroectoderm-derived pigment epithelium of the retina.

Autoradiographic analyses from sections of 11.5 fetus hybridized with the radioactive ET-B complimentary RNA probes revealed the expression of ET-B mRNA in heart, lung, liver, colon (Figure 2.3), pancreas, adrenal kidney, and skin. The observations were further confirmed with the use of non-radioactive biotin-labeled RNA probes on whole-mount preparation. Negative control experiments did not show any specific hybridization signals.

Skeletal examination using double staining method of C. Arrnot revealed skeleton was largely unaffected.

2.3.2 ET-B is allelic to the piebald locus

The phenotype of the homozygous ET-B mice closely resembled that observed in mice homozygous for the natural mutation piebald-lethal. The piebald locus has been mapped to region of mouse chromosome 14 (Metallinos et al., 1994) that is believed to be syntenic to human chromosome 13, where the ET-B gene maps in humans (Arai et al., 1993). These considerations led us to suspect that the piebald mutations may disrupt the ET-B gene. There are two known, naturally occurring mutant alleles in the piebald locus: a severe allele, , s^1, gives rise to megacolon and coat color spotting in homozygotes, whereas a mild allele, s, result in coat color spotting only. To test the above hypothesis directly, we intercrossed s/s^1 compound heterozygote mice (which manifest spotting only) with ET-B$^-$

/+ heterozygotes. Because both ET-B$^-$ and s (s^1) are recessive, the expression of a mutant phenotype in offspring from these intercrosses indicates that these loci are allelic. Out of the 13 offsprings obtained from two intercrosses, 6 showed the wild-type phenotype. These pups were inferred to carry the wild-type allele from the ET-B$^-$/+ parent. Out of 13 offspring, 3 exhibited mild spotting (40%-50% white body surface area) without manifesting megacolon at up to 60 days. This resembled the phenotype of the s/s^1 mice, and their genotype was presumably s/ET-B$^-$. This was compatible with the idea that the mild s allele is dominant over the null ET-B allele with respect to the megacolon phenotype. Finally, 4 out of 13 pups showed extensive white spotting, resembling the s^1/s^1 and ET-B$^-$/ET-B$^-$ mice (>90% body surface area). All of these 4 offspring eventually died from megacolon, and we inferred that the genotype of these mice was s^1/ET-B$^-$. These observations indicate that the ET-B$^-$ and s(s^1) alleles fail to complement each other, and therefore, ET-B is allelic to piebald. These findings also suggest that the s^1 allele is, like ET-B$^-$, a null or nearly null allele.

2.3.3 The entire ET-B gene is deleted in the piebald lethal (s^1) chromosome.

We confirmed the allelism between ET-B and piebald by analyzing the s^1/s^1 and s/s strains biochemically. As expected, kidney membranes from s^1/s^1 homozygotes did not show significant numbers of ET-B-binding sites. In contrast, membrane preparations from the s/s mice contained a detectable, but greatly reduced density of ET-B-binding sites. We next examined the expression of the ET-B mRNA in tissues that normally express relatively high amounts of the mRNA. The ET-B mRNA was undetectable by Northern blot analysis in all s^1/s^1 tissues examined. The expression of the ET-A mRNA was not appreciably altered in these mice. Furthermore, Southern blots showed that a DNA segment encompassing all of the coding exons of the ET-B gene was deleted in the s^1/s^1 genome. These findings, together with the identical phenotype of the ET-B$^-$/ET-B$^-$ and s^1/s^1 homozygotes, establish that the piebald gene encodes ET-B.

2.3.4 Attenuated ET-B mRNA expression from the piebald (s) allele

In s/s mice, northern blots revealed an ET-B$^-$ mRNA of normal size (4.5 kb) in the lung. However, the level of ET-B mRNA expression was markedly decreased in s/s lungs as compared with lungs from wild-type mice. The intensity of the s/s tissues was ~ 28% of that in the corresponding wild-type tissues, as quantitated with a phosphorimager after normalization with respect to the intensities of ß-action mRNA signals. To examine whether the ET-B mRNA is structurally abnormal in s/s mice, we cloned full-length ET-B cDNA from s/s and wild-type lungs by reverse transcription-PCR (RT-PCR) and determined the nucleotide sequence of the entire coding region. We detected two silent nucleotide substitution, which are considered to be polymorphisms between C57BL/6J and SSL/Lc strains. No alterations in the encoded amino acid sequence were observed in the s/s cDNA. Taken together, a decreased but not absent expression of structurally normal ET-B mRNA in the s/s tissues was compatible with the mild phenotype seen in the s/s homozygotes.

Figure 2.1. Gross Anatomical Phenotype of ET-B Null Mice.

(A) White-spotted coat color of a homozygous $ET\text{-}B^-/ET\text{-}B^-$ mouse (middle). An s^1/s^1 mouse (left) is almost completely white. An s/s mouse (right) exhibits less extensive spotting. Note the dark eyes of these mice.

(B) A cross between a heterozygous $ET\text{-}B^-/+$ female (top left) and a compound heterozygote s^1/s male (top right). Four of the pups from this cross (bottom, 1-4) are shown. Genotype of pups: 1 and 4, $ET\text{-}B^-/s$; 2, $ET\text{-}B^-/s^1$; 3, $+/s^1$ and +/s.

(C) Autopsy of wild-type (left) and $ET\text{-}B^-/ET\text{-}B^-$ (right) mice. An arrow indicates the distended colon in the homozygous mice.

(D) Dissection of the entire gastrointestinal tract from wild-type (left) and $ET\text{-}B^-/ET\text{-}B^-$ (right) mice. ST, stomach; CE, cecum. Dissension of the distal ileum, cecum, and proximal colon is evident in the ET-B/ET-B intestine. An arrow depicts the transitional zone between the proximal distended and distal narrow (aganglionic) segments of the $ET\text{-}B^-/ET\text{-}B^-$ colon.

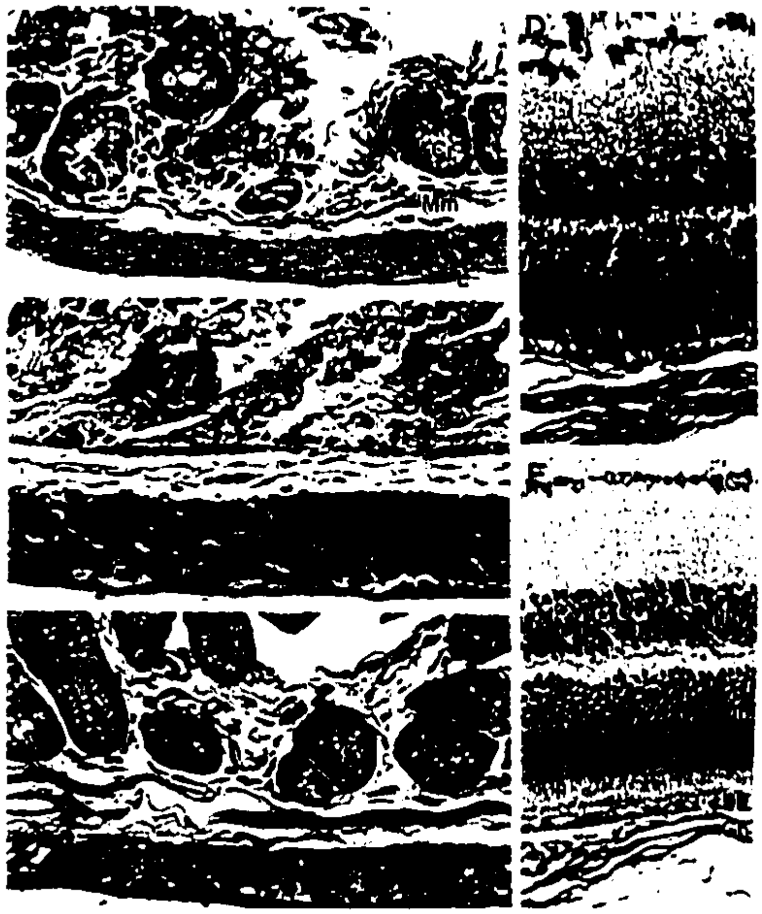

Figure 2.2. Histological Examination of Defects in ET-B Null Mice.

(A-C) Longitudinal sections of the distal (A) and proximal (B) colon from the same ET-B⁻/ET-B⁻ mouse and the distal colon from a wild-type mouse (C). Cr, crypts; Mm, muscularis mucousa; C, circular layer of muscle; L, longitudinal layer of muscle. Asterisks indicate myenteric (Auerobach) ganglia between the circular and longitudinal layers of muscle. The ganglia are absent from the distal segment of the ET-B⁻/ET-B⁻ colon (A). Note the inflammation and partial destruction of mucousa in the distended proximal segment of the ET-B⁻/ET-B⁻ colon (B) due to the severe ileus.

(D and E) Retina from the ET-B⁻/ET-B⁻ (D) and wild-type (E) mouse. G, ganglion cell layer; In, inner nuclear layer; On, outer nuclear layer; PE, pigmented epithelium; Ch, choroid. Choroidal melanocytes are absent from the ET-B⁻/ET-B⁻ retina. The melanin contents of the pigment epithelium appears normal in the ET-B⁻/ET-B⁻ retina.

Figure 2.3 In situ hybridization.

Expression of ET-B mRNA in wild type ET-B colon.

2.4 Discussion

The findings presented in this study establish ET-B as an essential component in the normal development of two neural crest-derived cell lineages, namely, enteric ganglion neurons and epidermal melanocytes. We did not detect a major anatomical abnormality in other tissues or a gross behavioral defect in the homozygous ET-B mice.

We have demonstrated that the entire ET-B gene is missing from the s^1 chromosome 14. At this time, we do not know the exact extent of the DNA deletion, or whether one or more adjacent genes are also deleted. The near identical phenotype of the homozygous ET-B and s^1/s^1 mice indicates that the deletion of ET-B is sufficient for the expression of both coat color spotting and the megacolon phenotype. In this regard, we observed a very subtle difference in the coat color phenotype between the homozygous ET-B and s^1/s^1 mice. the Homozygous ET-B mice almost always show small pigmented patches in the head and hip regions (<10% of body surface area), whereas the s^1/s^1 mice are almost completely white. We feel that this is due to the difference in genetic background between this strains, i. e., the hybrid 129/Sv C57B/6J background of the ET-B null mice versus the SSL/Lc background of the piebald-lethal mice. The influence of genetic background on the extent of white spotting in the piebald and other spotting mutants has been discussed extensively (Silvers, 1979). For example, the s/s homozygotes exhibit ~20% coat color spotting in the SSL/Lc background. However, when bred into a C3H/nonagouti background, the s/s mice present themselves as primarily black mice with only tiny white spots in the belly. In contrast, an s/s stock described by Mayer (Mayer,

1977) is extensively (>50%) spotted. these findings suggest the existence of other coat color-determining loci that interact with the ET-B gene. In addition, the random pattern of white spotting in individual mice (even under an inbred genetic background as in the case of s and s^1 strains) indicates the existence of a stochastic component that functions together with the ET-B gene to determine whether a given skin region is pigmented or not (Pavan and Tilghman, 1994).

We have demonstrated that the ET-B mRNA is structurally intact in terms of the overall length and coding region sequence in s/s mice. However, the expression of ET-B mRNA was decreased to approximately 28% of the wild-type levels in the s/s mice as assessed by Northern blots. This was also consistent with our finding that s/s homozygotes showed only ~ 27% of the ET-B density seen in wild-type mice as judged by radioligand binding assay. We speculate that a mutation in the regulatory regions of the ET-B gene, in its introns or in its noncoding exon sequence, results in a decreased level of mRNA expression. Considering that s^1 is a null allele, the relative ratio of ET-B expression in s^1/s^1, s/s^1, s/s, $s^1/+$, and +/+ mice is presumably about 0%: 12.5%: 25%: 50%: 100%. It is interesting to note that s^1/s^1, s/s^1, and s/s mice show a graded coat color phenotype in the extent of white spotting, having white coat in >95%, 40%-50% and about 20% of body surface area, respectively (Lane et al., 1966; Lyon and searle, 1989) (our experience confirmed these reports). These observations indicate that the extent of white spotting is precisely dependent on the dosage of ET-B expression. In contrast, the megacolon phenotype occurs only in the s^1/s^1 and $ET\text{-}B^-/ET\text{-}B^-$ homozygotes, both of which have zero ET-B expression, but almost never in the s/s^1 or s/s mice (Lane et al., 1966; Lyon and searle, 1989). This is compatible with the idea that the two neural crest-derived cell lineages required different minimal threshold levels of ET-B expression. Thus, about 12.5% of the wild-type levels of ET-B density is sufficient for the normal development of myenteric ganglion neurons, whereas 25%-50% of the wild-type level is required for complete development of epidermal melanocytes.

Further studies are needed to elucidate the exact development role of the regulatory signals transmitted via ET-B in neural crest-derived cell lineages. A previous study of piebald-lethal mice that employed a lineage specific marker for melanoblasts, tyrosinase-related protein 2 (TRP-2), has shown that the expression of TRP-2 was virtually restricted to the nonneural crest-derived melanocytes of retinal pigment epithelium and telencephalon in s^1/s^1 embryos by embryonic day 10.5 (Pavan and Tilghman, 1994). In W and Sl mutant embryos, TRP-2 positive cells were still present in reduced numbers in day 11 embryos (Steel et al., 1992). Taken together with the present findings, this indicates that the absence of signaling via ET-B disrupts development of the neural crest-derived melanocytes prior to the onset of TRP-2 expression. The detection of TRP-2 at a later development stage in W and Sl embryos than in s^1/s^1 embryos suggests that signaling via ET-B may function upstream of the interaction of the c-kit receptor and its ligand in melanoblast development. This situation seems to differ slightly in the myenteric ganglion neurons. A series of studies has been carried out by Kapur et al.(1992) with a lacZ receptor transgene driven by the neuroblast-specific dopamine B-hydroxylase promoter. A preliminary study showed that, in s^l/s^l embryos, neuroblasts migrated in a cranial-to-caudal direction, exactly identically to wild-type mice until they reached the ileocecal junction at embryonic day 11.5. At that point, further colonization of the large intestine was markedly impaired by the piebald-lethal mutation (R.P. Kapur, personal communication). These findings suggest that ET-B acts at much later stage in development of myenteric ganglia in comparison with epidermal melanocytes. Studies with earlier markers for neural crest cell lineages, such as c-ret (Pachnis et al., 1993) and Mash 1(Anderson et al., 1994), may further pinpoint the role of ET-B-mediated signaling in the development of these cells.

Mayer et al. have shown by cross-explanation of embryonic skin and neural crest that piebald acts in the neural crest (melanoblast) rather than in the skin (Mayer et al., 1977). He concluded that s/s melanoblasts possess a reduced proliferative capacity, leading to a failure of melanoblasts to occupy certain skin areas. This view of a cell-autonomous action of piebald predicts that the ET-B is expressed on melanoblasts, in which it mediates a proliferative or differentiation signal in these migratory cells. Indeed, several studies have shown that cultured melanoblasts and melanoma cell lines express ET-B and that endothelin agonists stimulate the proliferation and chemokinesis of these cells via ET-B (Yada et al., 1991; Yohn et al., 1994). In situ hybridization histochemistry also indicate that ET-B is expressed on migrating melanoblasts in wild-type mouse embryos. Human myenteric ganglion neurons have also been shown to express ET-B (Inagaki et al., 1991). This supports the notion that the piebald-lethal mutation acts cell autonomously in myenteric ganglion neurons. The present demonstration of the molecular basis of the piebald-lethal mutation should help to clarify the mechanism of migration and colonization of enteric neuroblasts in greater details.

The aganglionic megacolon seen in s^l/s^l and $ET\text{-}B^-/ET\text{-}B^-$ homozygous mice is considered to be pathophysiologically analogous to human Hirschprung's disease (HSCR). The region of mouse chromosome 14 in which piebald has been mapped (Metallinos et al., 1994) is thought to be syntenic to human chromosome 13, which harbors the human ET-B gene (Arai et al., 1993). A number of reports describe interstitial deletions of human chromosome 13 q associated with HSCR (Lamon et al., 1989). Furthermore, one of the genes responsible for a multigenic form of familial HSCR has recently been mapped to human chromosome 13q22 (Puffenberger et al., 1994a). These considerations implicate ET-B as a plausible candidate gene for HSCR. Indeed, it has been described a missense mutation of ET-B that is associated with the HSCR phenotype in a large, inbred Mennonite pedigree (Puffenberger et al., 1994b). Some of the individuals in this pedigree who are homozygous for the ET-B mutation manifest pigmentary disorders including white forelock, regional hypopigmentation of skin, and bicolored irides (type IV Waardenburg Syndrome). This indicates that ET-B plays an important role in the development of the two neural crest-derived cell lineages in humans as in mice. However, the genetics of ET-B show a number of important differences in the two species. First, in humans, the penetrance of the HSCR phenotype is incomplete in individuals homozygous for the ET-B missense mutation (Puffenberger et al., 1994b). Second, heterozygous human individuals are also at risk for aganglionic megacolon, although the risk is much lower than in homozygous individuals. These characteristics of inheritance are in sharp contrast to the situations in the mouse, in which s^l and ET-B alleles are both completely recessive to the wild-type allele and the coat color spotting and megacolon phenotypes exhibit 100% penetrance in homozygous animals. These discrepancies may partly be explained by the fact that the ET-B missense mutation in this human pedigree significantly impairs but dose not completely abolish signaling via ET-B, unlike the completely null mutations in s^l/s^l and ET-B$^-$/ET-B$^-$ mice, and also that other genetic loci, including the c-ret gene, are clearly involved in the HSCR susceptibility in this Mennonite pedigree (Puffenberger et al., 1994b). A similar species related difference in mode of inheritance exists in the case of c-ret mutations, which also produce enteric agangliosis. In the mouse, a targeted null mutation of c-ret leads to a recessive defect, with total agangliosis throughout the gastrointestinal tract in homozygous (Schuchardt et al., 1994). In contrast, loss-of-function c-ret mutations, including those are thought to be functionally null, result in a dominant HSCR phenotype in humans probably due to haploinsufficiency (Fisher and Scambler, 1994; Romeo et al., 1994).

ET-B receptor accepts all three endothelin isopeptides with similar affinities (Sakuria et al., 1990; Yanagisawa, 1994). Which isopeptide is the physiologically relevant ligand in the development of neural crest-derived melanocytes and enteric neurons? In the next part of this project, we demonstrate that mice deficient for endothelin 3 exhibit the identical phenotype of white [illegible] and megacolon. These findings establish that endothelin-3 is the relevant ligand. Our results indicate that interaction of ET-3 with the endothelin-B receptor is essential in the development of neural crest-derived cell lineages.

Chapter 3

Role of the Endothelin-3 Gene in Normal Development

3.1 Introduction

In chapter 2, we have demonstrated that ET-B receptor plays an essential role in the normal development of epidermal melanocytes and enteric ganglion neurons in mice and humans. Mice homozygous for a knocked-out ET-B allele exhibited white-spotted coat color associated with aganglionic megacolon, a phenotype closely resembling the defects seen in three natural mouse mutants, piebald-lethal (s^l), lethal spotting (ls), and dominant megacolon (DOM) (Lyon and Searle, 1989). We demonstrated that the piebald locus indeed encodes ET-B. Although all three endothelin isopeptides can bind and activate ET-B receptor equally, the phenotype observed in these mice was clearly different from that seen in the ET-1 knockout mice (Kurihara et al., 1994). In the present study, we demonstrate that ET-3-deficient mice exhibit an identical phenotype of coat color spotting and aganglionic megacolon. We further show that lethal spotting is allelic to the mouse ET-3 gene. We also identify a missense mutation of the ET-3 gene in the ls/ls mice. Although the mutation leaves the mature ET-3 sequence intact, it abrogates the production of mature peptide by ECE-1 in these animals.

Note: This part of project was done in a collaborative work with Howard Hughes Medical Institute and Department of Molecular Genetics in Dallas, Texas.

3.2 Experimental procedures

3.2.1 Mutant mouse strains

LS/Lc ls/ls males and LS/Lc ls/+ females are purchased as breeding pairs from The Jackson Laboratory.

3.2.2 Production of ET-3-deficient mice

The mature ET-3 sequence resides in the middle portion of the prepro-ET-3 polypeptides and is encoded by exon 2 of the mouse ET-3 gene. To introduce an ET-3 null mutation by homozygous recombination in mouse embryonic stem (ES) cells, a replacement vector was constructed, in which the mature ET-3-encoding portion of ET-3 exon 2 is substituted by a neomycin resistance cassette (neo) as described in chapter 2 (2.2.2). Briefly, herpes simplex virus thymidine kinase(TK) cassettes were added to the 3' end of the targeting vector for positive-negative selection. Screening of 108 double-resistant cell clones by PCR revealed nine homologous recombinant clones. Southern blot analysis confirmed that these clones had a correctly targeted ET-3 allele. Five of the recombinant ES cell clones of ET-3 gene were injected into C57BL16J blastocysts, and four of these clones yielded male chimeric mice that transmitted the targeted allele through the germline.

3.2.3 Histology

Mice were perfusion fixed with formalin immediately after sacrifice, and tissues were dissected and further immersion fixed in formalin. Embedded tissues were cut into 5 μm sections and stained with hematoxylin and eosin by a standard procedure that described in chapter 2 (2.3.3). Sections were then examined under bright-field microscopy.

3.2.4 Skeletal examination

The tissues were fixed in 80% ethanol for 24 hrs and dehydrated in 96% ethanol for 24 hrs and then acetone for 3 days. For skeletal examination, the double staining method of C. Arrnot, that described in chapter 2 (2.2.4), was used. Briefly, tissues were stained with alcian blue and alizarin red for bone and cartilage examinations. The tissues were stored in 100% glycerin.

3.2.5 In situ hybridization

In situ hybridization was carried out by a modification of a method reported previously (Giaid et al., 1991). The method completely described in chapter 2 (2.2.5) Briefly, the tissues were fixed in paraformaldehyde and cut with a cryostat. ET-3 probes were then labeled using ^{35}S-UTP.

3.2.6 Radioligand binding assay

Kidney membrane fractions were prepared from freshly sacrificed mice as described (Bolger et al., 1990). Binding assay was carried out as described in chapter 2 (2.2.6) with 10^{-11} M[^{125}I] endothelin-1 as tracer and using 30 μg of membrane protein per reaction.

3.3 Results

3.3.1 pigmentary disorder in homozygous ET-3 null mice.

We did not detect any abnormality in heterozygous F2 mice. An extensive white spotting of the skin and coat in homozygous ET-3 mice apparent by days 3-4 postpartum (Figure 3.1 A). About 70%-80% of the coat was completely white. Well-demarcated, normally pigmented patches of coat were seen most often in the head and hip regions. The shapes of these pigmented patches are irregular and differ at random from mouse to mouse. In comparison with the ET-B null mice, the degree of white spotting in the homozygous ET-3 mice was appreciably milder. We often observed a large, continuous patch of pigmented coat in the head and hip of homozygous ET-3 mice, which were rarely found in the homozygous ET-B mice. The belly was almost always white. The eyes are dark in all homozygotes.

Histological examination of the skin sections taken from the spotted region of homozygous ET-3 mice confirmed the absence of melanin pigment in the coat hair and the absence of melanocytes in hair bulbs. In these skin sections, we did not see "amelanotic melanocytes" or clear cells, which are often found in the hair bulbs of albino mice. In the skin sections taken from the pigmented region of homozygous ET-3 mice, the amount of melanin pigment and the number of melanocytes appeared normal. These findings are consistent with the idea that depigmentation in homozygous ET-3 mice is not due to an inability of melanocytes to synthesize melanin (as in the case of albino mice), but to a regional failure of melanocyte colonization in the skin. Sections of the homozygous ET-3 eyes revealed an absence of melanin pigment in the choroidal layer of the retina (Figure 3.2 A). By contrast, the melanin content in the retinal pigment epithelium appeared normal, consistent with the dark eyes of the homozygotes mice. In the wild-type retina, both layers of melanin pigment were clearly observed (Figure 3.2 B). These findings are consistent with the idea that the homozygous ET-3 mice have defect in the development of neural crest-derived melanocytes but not in the neuroectoderm derived retinal pigment epithelium.

3.3.2 Aganglionic megacolon in ET-3 null mice

Other than the spotted coat color, homozygous ET-3 mice appeared healthy in the first few days after birth, and we did not detect a gross behavioral abnormality. Within the first month after birth, however, most of the homozygous mice became increasingly sick, and they eventually died. The disease-free period varied greatly. Out of 44 randomly chosen mice, 6 died by day 7, 16 by day 14, 40 by day 30, and 43 by day 65. The mean and median life span of these 43 animals were 21 days and 19 days, respectively (range, 4-65 days). One homozygote lived to mate and eventually died on day 85. We performed an autopsy on at least 30 of the ET-3 null mice, which were sacrificed 1-2 days before they would have died. In all animals examined, we observed a gross distension of the intestine (Figure 3.1 B). Upon dissection of the entire gastrointestinal tract, we found that the distal large intestine was narrow. The narrow segment was directly preceded by a distended proximal segment (Figure 3.1 C). This gross appearance was consistent with the diagnosis of aganglionic megacolon. The spastic portion included the most distal part of the rectum in all cases. However, the position of the transitional zone between the distended (proximal) and spastic (distal) segment varied from animal to animal. In some homozygotes, the entire colon appeared narrow (microcolon). In others, only the most distal 2-3 mm of the rectum was spastic, resulting in distension of the entire colon. The spastic segment most often spanned from the sigmoid colon to the distal rectum. The length of the spastic segment and the life span of the animal did not appear closely correlated.

The absence of myenteric ganglia in the distal narrow segment of the colon was confirmed in histological sections from all 8 homozygous ET-3 animals examined (Figure 3.2 C). We observed apparently normal myenteric ganglion neurons between the longitudinal and circular layers of smooth in the proximal, distended segment of the homozygotes colon. Ganglion cells were seen in the entire length of the colon from age-matched wild-type animals (Figure 3.2 D).

Autoradiographic analyses from sections of 11.5 fetus hybridized with the radioactive ET-3 complimentary RNA probes revealed the expression of ET-3 mRNA in heart, lung, liver, colon, pancreas, adrenal, kidney, and skin (Figure 3.3). The observations were further confirmed with the use of non-radioactive biotin-labeled RNA probes on whole-mount preparation. Negative control experiments did not show any specific hybridization signals.

Skeletal examination revealed skeleton was largely unaffected.

3.3.3 *The lethal spotting locus encodes ET-3*

The recessive phenotype of the homozygous ET-3 mice closely resembled the syndrome manifested by two natural recessive mutations in the mouse, piebald-lethal and lethal spotting (Anderson et al., 1994). Lethal spotting has been mapped to a distal portion of mouse chromosome 2 (Lyon and Searle, 1989), which harbors the human ET-3 gene (Arinami et al., 1991). These findings strongly suggested that the ET-3 gene may be allelic to lethal spotting. To test this directly, we examined whether the recessive ET-3 and ls mutations can complement each other. It has been known that some homozygous ls/ls mice survive to mate and give rise to offspring, without manifesting terminal illness. We intercrossed two ls/ls males who had not manifested an overt megacolon phenotype with three heterozygous ET-3$^-$/+ females, as well as with the single homozygous ET-3 female that had survived to mate. Out of 24 offsprings from the three ls/ls ET-3$^-$/+ crosses, 15 were spotted and the remaining 9 appeared wild-type; we inferred the genotype of these pups as ls/ET-3$^-$ and ls/+, respectively. All of the 15 spotted pups eventually died of megacolon by day 125 postpartum. This demonstrates that ET-3 cannot complement ls, and therefore, they are allelic. As expected, all of the 8 offsprings from the ls/ls ET-3$^-$/ET-3$^-$ intercross were spotted, and 7 of them died of megacolon by day 102 postpartum. Taken together with the identical phenotype of the ls/ls and ET-3$^-$/ET-3$^-$ homozygotes, these results show that lethal spotting disrupts the ET-3 gene.

3.3.4 A missense mutation of ET-3 gene in ls/ls

To dissect the molecular basis of the ls mutation further, we first determined tissue concentration of immunoreactive mature ET-3 in the ls/ls mice. Three different tissues from homozygous ls/ls mice did not contain a detectable amount of mature ET-3. Heterozygous ls/+ animals had 36%-76% of the wild-type tissue levels of mature ET-3, which were comparable to those seen in the ET-3$^-$/+ mice. This indicates that the ls mutation abrogates production of mature ET-3. We next compared the expression of ET-3 mRNA in tissues from ls/ls and wild-type mice. Northern blots of three tissue s that express relatively high amounts of ET-3 mRNA showed that the level of ET-3 mRNA expression in the ls/ls mice was identical to that in the wild-type animals. This indicates that the ls mutation does not impair production of ET-3 mRNA.

We then examined whether the ET-3 mRNA is structurally altered in the ls/ls mice. We cloned ET-3 cDNAs from wild-type and ls/ls mice by reverse transcription-PCR (RT-PCR) and determined the nucleotide sequence of the entire prepro-ET-3 coding region. In the ls/ls cDNA, we found a missense C→ T change in nucleotide 409 of the coding region, which results in a substitution of an Arg-137 residue (codon: CGG) with a Trp residue (codon: TGG). This mutation eliminates an XmnI restriction site (nucleotides 400-406), producing a convenient restriction polymorphism for genotyping the ls allele. We found no other sequence alterations in the ls/ls mRNA except for a silent C → A substitution of nucleotide 597 of the ET-3 coding region, which is considered to be an interstrain polymorphism.

3.3.5 The ls mutation abolishes production of active ET-3 by ECE-1

The R137W mutation was found within the highly conserved c-terminal portion of the big ET-3 sequence. The mutation replaces the first Arg residue of a tetrapeptide sequence RGKR, which is believed to be the signal recognized by a furin-type prohormone-processing enzyme (Barr,1991). The GKR sequence that immediately follows Arg-137 matches the consensus sequence for c-terminal peptide amidation (Eipper et al., 1993). Indeed, human big ET-3 has recently been shown to be amidated at the C-terminal Arg residue (Kosaka et al., 1994). Thus, furin or a similar processing enzyme recognizes the tetrapeptide RGKR sequence and cleaves after Arg-140. Then, a peptidylglycine-amidation enzyme forms Arg-137 amide by cleaving between the α carbon of Gly-138 and the main-chain amido group in the N-terminal side of Gly-138.

Since we did not detect immunoreactive ET-3 in the ls/ls tissues, we postulated that the R137W mutation abrogates the formation of mature ET-3, even though the mutation leaves the mature ET-3 sequence itself intact. To examine the role of the mutation directly, we tested whether transfection of wild-type and mutant ET-3 cDNA leads to secretion of mature ET-3 into the culture medium. We subcloned the prepro-ET-3 coding sequence from the wild-type and ls/ls cDNAs into an expression vector and transfected the constructs into CHO/ECE-1 cells (Xu et al., 1994). This cell line expresses ECE-1, which can specifically cleave big ET-3 into the mature peptide. CHO/ECE-1 cells transfected with wild-type ET-3 cDNA secreted immunoreactive big ET-3 as well as mature ET-3 into the medium. In contrast, cells transfected with the R157W mutant cDNA did not produce a significant level of mature ET-3. However, these cells produced similar amounts of immunoreactive big ET-3 indicating that the mutation does not abolish the production of the precursor peptide.

Figure 3.1. White Spotting and Megacolon in ET-3-Deficient Mice.

(A) Coat color spotting in a homozygous ET-3 mouse (right) and on ls/ls mouse (left). Note the large, continuous pigmented patches in the head and hip regions of these mice.

(B) Autopsy of wild-type (top) and homozygous ET-3 (bottom) mice. An arrow indicates the distended ileum of the homozygous ET-3 mice.

(C) Dissection of the entire gastrointestinal tract from wild-type (right) and homozygous ET-3 (left) mice. St, stomach; Ce, cecum. Distension of the ileum and cecum is evident in the homozygous ET-3 intestine. In this particular mouse, the entire colon was aganglionic.

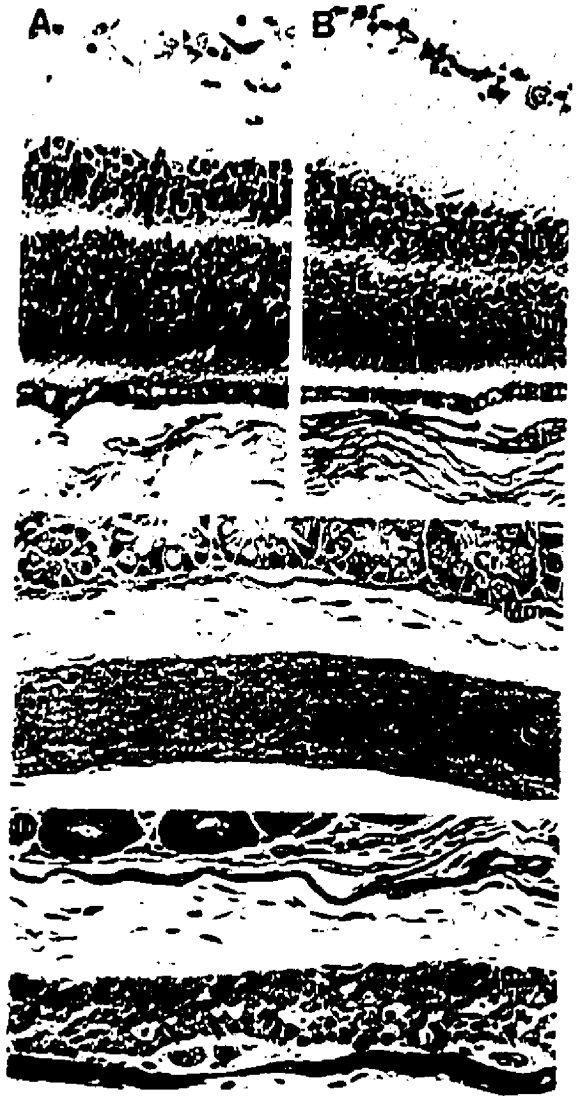

Figure 3.2. Homozygous ET-3 Mice Lack Retinal Choroidal Melanocytes and Myenteric Ganglion Neurons.

(A and B) Retina from the homozygous ET-3 (A) and wild-type (B) mouse. G, ganglion cell layer; In, inner nuclear layer; On, outer nuclear layer; PE, pigment epithelium; Ch, choroid. The pigment epithelium appears normally pigmented in the homozygous ET-3 retina, but the choroidal pigmentation is absent.

(C and D) Longitudinal sections of the distal colon from homozygous ET-3 (C) and wild-type (D) mice. Cr, crypts; Mm, muscularis mucousa; C, circular layer of muscle; L, longitudinal layer of muscle. Arrowheads in (D) indicate myenteric (Auerbach) ganglion neurons between the circular and longitudinal muscle layers of the wild-type colon. The ganglia are absent from the homozygous ET-3 colon (C).

Figure 3.3 In situ hybridization.

Expression of ET-3 mRNA in wild type mouse skin.

3.4 Discussion

In this study, we have demonstrated that ET-3 plays an essential role in the normal development of these two neural crest-derived cell lineages, epidermal and choroidal melanocytes and enteric ganglion neurons. In chapter 2, we have shown that ET-B receptor is also essential for development of two cell lineages. The three known mammalian isopeptides, ET-1, ET-2, and ET-3, all function as potent agonists for ET-B receptor. These isopeptide ligands have similar affinities and efficacies toward ET-B receptor (Sakuria et al., 1990). The present findings establish that the signal conveyed by ET-3 via ET-B receptor is specifically required in the development of these cells.

The homozygous ET-3 animals had normal tissue levels of immunoreactive mature ET-1 plus ET-2. This indicates that these isopeptides cannot compensate for the function of ET-3 in the development of epidermal melanocytes and enteric ganglia. These findings suggest that endothelin isopeptides do not function as circulating hormones, even though they are produced as small soluble molecules. If they did act as systematically circulating peptides, ET-1 (or ET-2) could have compensated for the lack of ET-3, since ET-B receptor accepts all three isopeptides equally and the plasma and tissue levels of ET-1 are generally higher than those of ET-3 (Matsumoto et al., 1989; Suzuki et al., 1990). There is the formal possibility that ET-1 (or ET-2) is available to ET-B receptor but that different endothelin isopeptides produce different intracellular signals upon binding to ET-B receptor. For example, binding of different endothelins to ET-B receptor might induce the receptor to interact with different classes of G proteins. However, there is no known example for such multiple differential modes of receptor activation. One trivial explanation might be that ET-1 and ET-2 are not expressed during embryonic lives. However, homozygous ET-1 knockout mice die shortly after birth due to craniofacial abnormalities involving the first branchial arch-derived tissues (Kurihara et al., 1994). In situ hybridization confirmed that ET-1 is expressed in the first branchial arch in the wild-type embryos. It is not clear whether ET-1-deficient homozygotes had any abnormalities in epidermal melanocytes or enteric neurons, since these defects do not become obvious until a much later time (e.g., until days 3-4 postpartum for skin color spotting). However, the strikingly similar phenotype of the homozygous ET-B and homozygous ET-3 mice suggests that the absence of ET-3 is sufficient to reproduce ET-B null phenotype and that ET-1 or ET-2 dose not play a major role in development of these two cell lineages.

In this regard, we observed that the phenotype of homozygous ET-3 and ls/ls mice was appreciably milder than that of the homozygous ET-B and s^l/s^l mice. The homozygous ET-B mice were >90% white and the s^l/s^l almost completely white. In contrast, the homozygous ET-3 and ls/ls mice usually had pigmented coat in 20%-30% of body surface area, often as large pigmented belts in the head and hip regions, sometimes giving a panda-like appearance. With regard to the megacolon phenotype, none of the homozygous ET-B mice survived to mate, and s^l/s^l mice in SSL/Le background has been reported almost never to survive to mate (Lane, 1966; Lyon and Searle, 1989). In contrast, ~ 15% of homozygous ET-3 and ls/ls mice as well as the ls/ET-3 mice survived well beyond adulthood. These differences cannot be explained by an incomplete nature of the mutation or by difference in genetic background.Homozygous ET-B, s^{l}, and homozygous ET-3 are all null alleles. We have demonstrated that the ls allele is also functionally null, although we cannot exclude the possibility that mature ET-3 was produced in the ls/ls animals at an extremely low level that was below our detection limit. There was no systematic difference in genetic background between the homozygous ET-3 and homozygous ET-B strains, both of which had a hybrid 129/Sv C57BL/6J background. We feel that the milder phenotype seen in the ET-3 mutant mice in comparison with the ET-B mutants is due to a small degree of compensation by diffusible ET-1 and ET-2 that are produced in nearby or remote embryonic tissues, or possibly by endothelin isopeptides carried over from the maternal circulation.

We have demonstrated that CHO/ECE-1 cells transfected with the R137W/ (ls) mutant ET-3 cDNA did not produce mature ET-3. Significantly, however, the production of immunoreactive big ET-3 was not affected by the mutation. The sandwich EIA for big ET-3 used in this study recognizes peptides that carry both an epitope in the N-terminal loop region of ET-3 and another epitope within the c-terminal 20 amino acids of big ET-3 (Matsumoto et al., 1989). Therefore, this EIA cannot distinguish between fully processed big ET-3 and larger precursor peptides. The prepro-ET-3 contains two consensus recognition sequences for the prohormone-processing enzyme furin, (K/R)x(K/R)R↓, immediately before and after the big ET-3 sequence. This predicts that furin or a similar processing enzyme first produces big ET-3 from (pre)pro-ET-3, which is then cleaved to mature, active ET-3 by ECE-1 or other enzyme(s) with big endothelin-converting activity

(Fabbrini et al., 1993; Xu et al., 1994). The R137W mutation disrupts the furin recognition sequence, RGKR, at the c-terminus of big ET-3 by substituting the first Arg residue that is at the P4 position with respect to the furin cleavage site. Previous studies with natural and site-directed mutants of various furin substrates have demonstrated that, for those substrates with a P4 basic residue, replacement of this residue with a nonbasic amino acid fully inhibits processing in vivo (Barr,1991; Bentley et al., 1986). Therefore, it is plausible to assume that the R137W mutant prepro-ET-3 cannot be cleaved at the c-terminus of big ET-3. In this case, the big ET-3 immunoreactivity we detected from the R137W ET-3-transfected cells was an incompletely processed precursor of big ET-3 with a c-terminal extension. Alternatively, the R137W mutant may still be cleaved by a processing enzyme with a less stringent recognition sequence, e.g., the basic pair site (K/R)R (Barr, 1991; Steiner et al., 1992). In this later case, the big ET-3 immunoreactivity we detected might have been a fully processed, 41 residue big ET-3 that had a point mutation at its very C-terminus. In either cases, our results demonstrate that the mutant big ET-3 (or its bigger precursor) cannot be further cleaved by ECE-1 to become mature, active ET-3. This is of interest because the ECE-1 cleavage site is 20 amino acids upstream from the mutated Arg residue. In this regard, we and others have previously shown that the c-terminal part of big ET-1 harbors an important structure for ECE-1 recognition (Okata et al., 1993; Xu et al., 1994). Collectively, these findings indicate that the ls mutant allele generates a c-terminal mutated (or aberrantly extended) big ET-3, which cannot be recognized by ECE-1 for the subsequent proteolytic activation. This results in the failure of mature ET-3 production observed in the ls/ls mice.

Previous studies using cross-explanation of embryonic skin and neural crest demonstrated that lethal spotting acts in the neural crest, which generates migrating melanoblasts, rather than in the skin, which provides an appropriate environment (Mayer, 1977). Similar studies with the piebald mice showed that s also is melanoblast autonomous. Taken together with the present findings, these observations are consistent with a model in which both ET-B receptor and ET-3 ligand are expressed in the neural crest-derived melanoblasts and function as an autocrine signal to maintain the proper migration and colonization of these cells. By contrast, previous studies on the migration of enteric neurons in ls/ls mice have led to quite different conclusions. Two independent studies have been conducted that employed aggregation chimeras between wild-type embryos and ls/ls embryos that were labeled with either transgenic or endogenous markers (Kapur et al., 1993; Rothman et al., 1993). Both studies demonstrated that, in the aggregation chimeras, the labeled ls/ls neuroblasts normally migrate (together with the unlabeled wild-type neuroblasts) to the distal end of the rectum, supporting the idea that the defect caused by the ls mutation is not neuroblasts autonomous. However, the present finding that ls encodes the diffusible extracellular factor ET-3 may complicate the interpretation of these previous results. For example, these studies cannot exclude the possibility that wild-type neuroblasts rescue nearby ls/ls neuroblasts by secreting ET-3 (Kapur et al., 1993). Unfortunately, analogous studies with s^1/s^1 embryos have not yet been carried out.

In chapter 2, we have demonstrated that defects in the ET-B receptor gene can result in pigmentary disorder and aganglionic megacolon in humans as well as in mice

(Hosoda et al., 1994; Puffenberger et al., 1994 b). Puffenberger et al. have identified a missense point mutation in the human ET-B receptor gene in patients with a hereditary form of Hirschsprung's disease (Puffenberger et al., 1994). The near-identical phenotype of aganglionic megacolon and white spotting shared by the homozygous ET-B (s^1/s^1) and homozygous ET-3 (ls/ls) mice, which carry defects in the interacting pair of cell surface receptor and extracellular ligand, points to the possibility that defects in human prepro-ET-3 gene may also cause Hirschsprung's disease. Our findings indicate that the interaction of ET-3 with ET-B receptor is essential for the normal development of two additional neural crest cell lineages, the vagal neural crest-derived enteric neurons and the trunk neural crest-derived epidermal melanocytes. The endothelins emerge as important regulators of mammalian neural crest development.

Chapter 4

Role of the Endothelin-A Receptor Gene in Normal Development

4.1 Introduction

To induce its numerous effects on smooth muscle contraction and stimulation of the release of autocoids and peptides, ET acts directly on specific receptors. Two types of G protein-coupled ET receptors have recently been described: ET-A and ET-B (Arai et al., 1990; Sakuria et al. 1990; Sakomoto et al., 1993). According to the relative binding affinities and biological activities of the three isopeptides for their receptors, ET-1 is equipotent to ET-2 but more potent than ET-3 on systems containing ET-As, whereas ET-1 is equipotent to ET-2 and ET-3 for the ET-B type (Ihara et al., 1992). The receptors which are responsible for the vasoconstrictive effects of ET have been identified as ET-As.

The human ET-A receptor genomic DNA has been cloned and characterized (Hosoda et al., 1992). Human ET-A gene present on chromosome 4, contains eight exons and seven introns. Introns 2 to 7 of ET-A occur within the coding region immediately proceeding or following one of the transmembrane helix domains, suggesting that the corresponding exons may encode functional units.

In the present study, after disrupting the ET_A gene in mouse ES cells to produce mice deficient in ET-A, we examined the phenotype of ET-A deficient mice to elucidate the physiological role of ET-A gene demonstrating that the mutation in the ET-A gene causes abnormal manifestation in fetal development.

Note: This part of project was done in a collaborative work with Howard Hughes Medical Institute and Department of Molecular Genetics in Dallas, Texas.

4.2 Experimental procedures

4.2.1 Targeted disruption of mouse ET-A gene

To introduce an ET-A null mutation by homozygous recombination in mouse embryonic stem (ES) cells, a replacement vector was constructed, in which the mature ET-A is substituted by a neomycin resistance cassette (neo) as described in chapter 2 (2.2.2). Briefly, herpes simplex virus thymidine kinase (TK) cassettes were added to the 3' end of the targeting vector for positive-negative selection. Screening of double-resistant cell clones by PCR revealed nine homologous recombinant clones. Southern blot analysis confirmed that these clones had a correctly targeted ET-A allele.

4.2.2 Histology

Mice were perfusion fixed with formalin immediately after sacrifice, and tissues were dissected and further immersion fixed in formalin. Embedded tissues were cut into 5 μm sections and stained with hematoxylin and eosin by a standard procedure that described in chapter 2 (2.3.3). Sections were then examined under bright-field microscopy.

4.2..3 *Skeletal examination*

For skeletal examination, the method of C. Arnott was used. The tissues were fixed in 80% ethanol for 24 hrs and dehydrated in 96% ethanol for 24 hrs and then acetone for 3 days. Staining was carried out for 6 hrs using the following solution: 0.1% alizarin red S in 95% ethanol (1 ml) and 1% acid-alcohol (99 ml). The tissues were cleared with 96% ethanol for 1 hr, 1% aqueous KOH for 48 hrs and 50% glycerin in 1% aqueous KOH for 2 weeks. The tissues were then stored in 100% glycerin

4.2.4 *In situ hybridization*

In situ hybridization was carried out by a modification of a method reported previously (Giaid et al., 1991). Briefly, the tissues were fixed in paraformaldehyde and cut with a cryostat. ET-A probes were then labeled using ^{35}S-UTP.

4.3 Results

Mice heterozygous for the ET-A mutation appear normal and were fertile. Although the heterozygous and wild-type newborn mice began to breathe and turn pink within 10 min. after birth, none of homozygotes opened their mouths to breath, and all responded poorly tapping and pinching stimuli. They remained blue and eventually died of anoxia within 15-30 min. examination of their lungs showed that they had never been ventilated.

4.3.1 Morphology of ET-A homozygous mice

In all of ET-A homozygous newborn mice examined, the same pattern of conspicuous craniofacial abnormalities was found. The mandible was poorly developed and its fusion in the midline was incomplete in the homozygous newborns. In addition, the anterior neck was thin and auricles were hypoplastic. These abnormalities were found in none of heterozygous or wild-type mice (Figure 4.1).

Histological examination revealed that homozygous mice, when compared to heterozygous and wild-type newborns had several morphological abnormalities particularly in the head and neck regions. Hyoid bone was smaller than that of wild-type or heterozygous. The anterior neck was thin and the mandible, submandibular glands, muscle and connective tissue were poorly developed. As well, the mandible fusion in midline was incomplete. Nasopharynx and oropharynx were narrow, but the lower airway appeared to be normal (Figure 4.2). Most of the tongue was missing, however the basal region remained and appeared hypertrophic. The muscle fibbers were irregular (Figure 4.3). In the outer ear, the auricles (pina) were hypoplastic and external auditory meatus was absent. In the middle ear, the incus and malleus were absent, but the stapes were missing (Figure 4. 4). The inner ear appeared to be intact. No ossification of the mandible condyle was seen, and the primitive gum and teeth were missing. Basiosphenoid bone was malformed

(Figure 4.5). In some homozygous, the ventricle wall of the heart appeared hypertrophic, and endocardial cushion defect was visible (Figure 4.6).

Examination of the skeleton with Alizarin red staining revealed that homozygous were lacking the tympanic ring, the auditory ossicle, and lower incisor tooth. Maxillary, premaxillary and hyoid bones were smaller than those of wild-type. Mandibular bone was retarded (Figure 4.7). Zygomatic bone was aberrant, and an extra bony protuberance in the thyro-hyoid region and also mandibular region was seen (Figure 4.8). Other parts of the skeleton were largely unaffected.

Autoradiographic analyses from sections of 11.5 fetus hybridized with the radioactive ET-A complimentary RNA probes revealed the expression of ET-A mRNA in mandibular components of first branchial arch (Figure 4.9), medial nasal process, submandibular glands, endocardial cushion tissue lining the atrioventricular canal, and in midline dorsal aorta. The observations were further confirmed with the use of non-radioactive biotin-labeled RNA probes on whole-mount preparation. Negative control experiments did not show any specific hybridization signals.

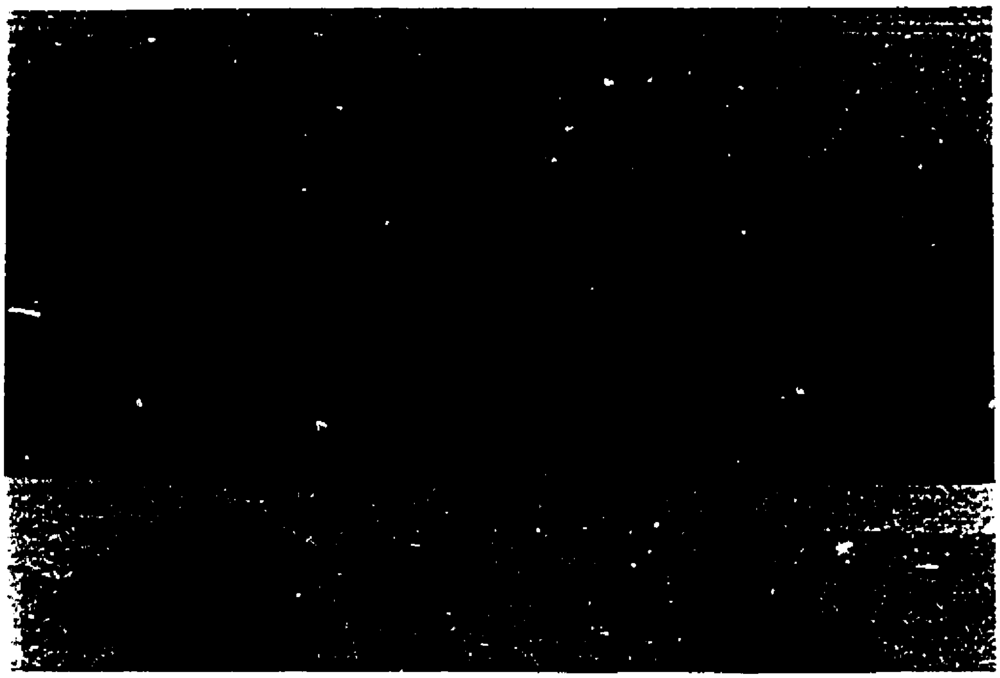

Figure 4.1. Comparison of Gross Anatomical Phenotype of ET-A Homozygous (a and c) and ET-A Wild-type (b and d) Mice. Homozygous mouse shows short and non-fused mandible (big arrow), thin anterior neck (small arrow), and hypoplastic auricles (arrowhead).

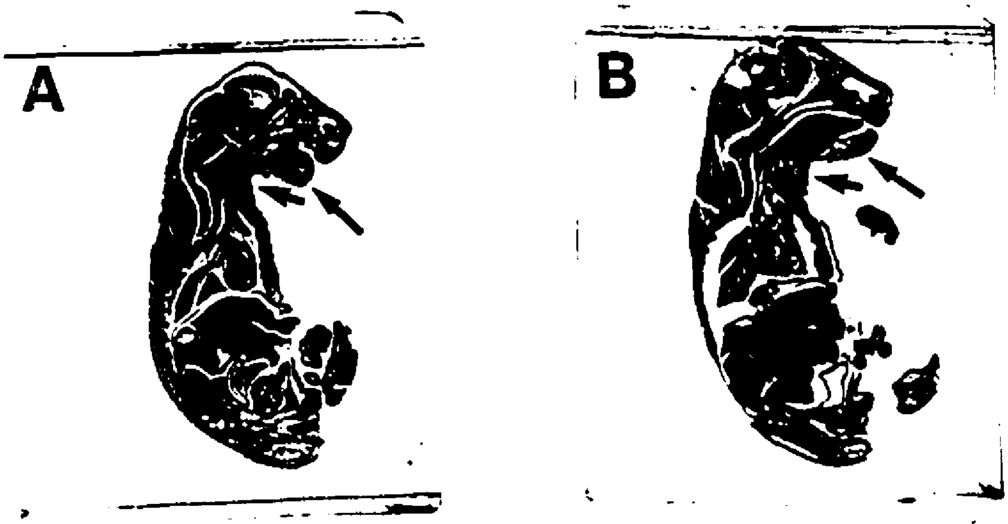

Figure 4.2. Whole Body Sections (sagital) of ET-A Homozygous (A) and ET-A Wild type (B) Mice. Homozygous mouse shows a short and non-fused mandible (big arrow), thin anterior neck (small arrow), small and hypertrophic tongue (T), as well as narrow upper airway (arrowhead).

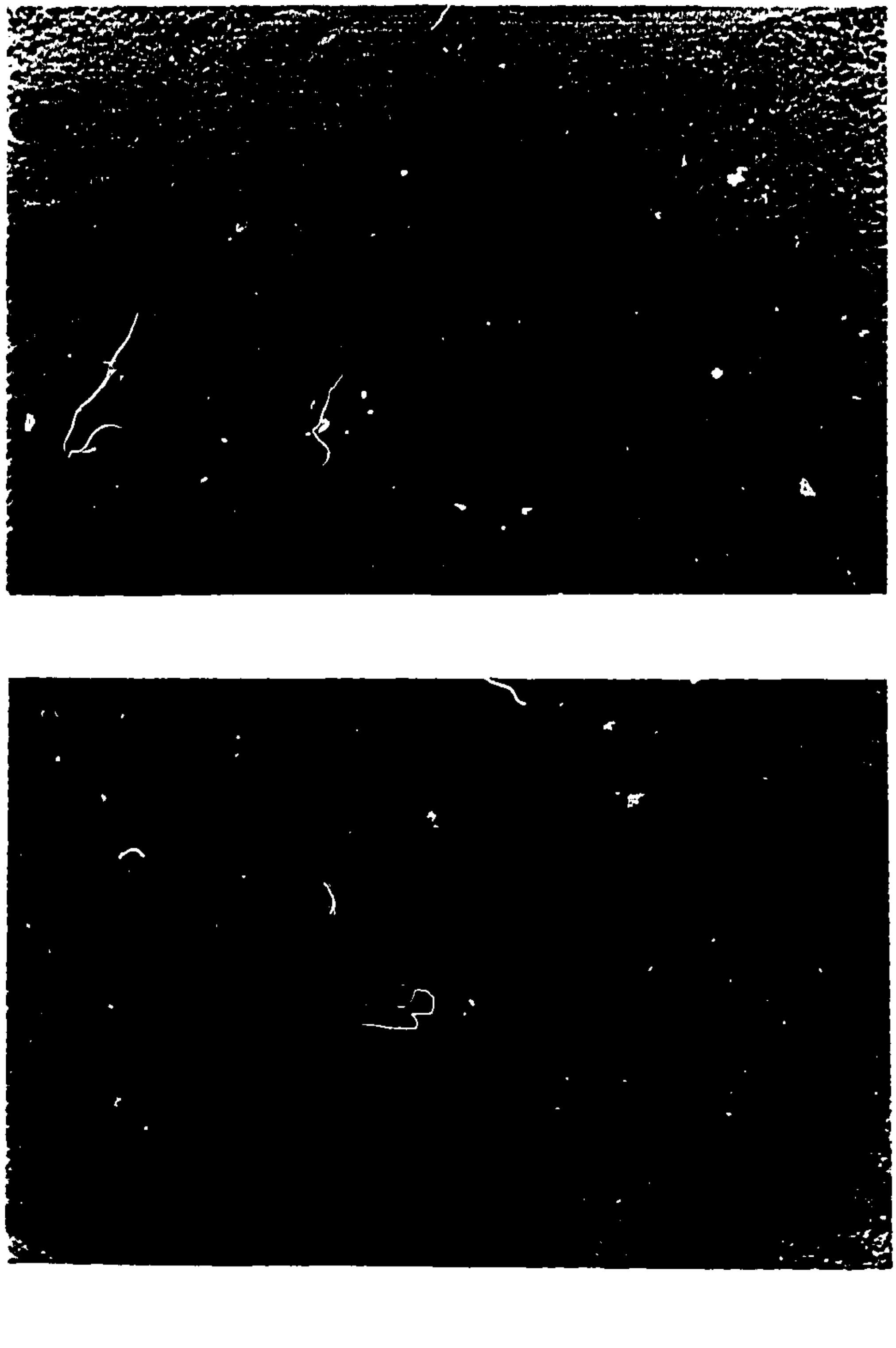

Figure 4.3. Comparison of Tongue Sections of ET-A Homozygous (A) and ET-A Wild-type (B) Mice. Tongue muscle fibers in ET-A homozygous mouse are irregular.

Figure 4.4. Comparison of Middle Ear Sections of ET-A Homozygous (A) and ET-A Wild-type (B) Mice. Malleus (big arrow) incus (small arrow), and stapes (arrowhead) in ET-A wild-type mouse are intact. In ET-A homozygous mouse, malleus and incus are intact, but stape is missing.

Figure 4.5. Head Section of ET-A Homozygous Mouse.

In ET-A homozygous mouse, basiosphenoid bone (arrow) is malformed.

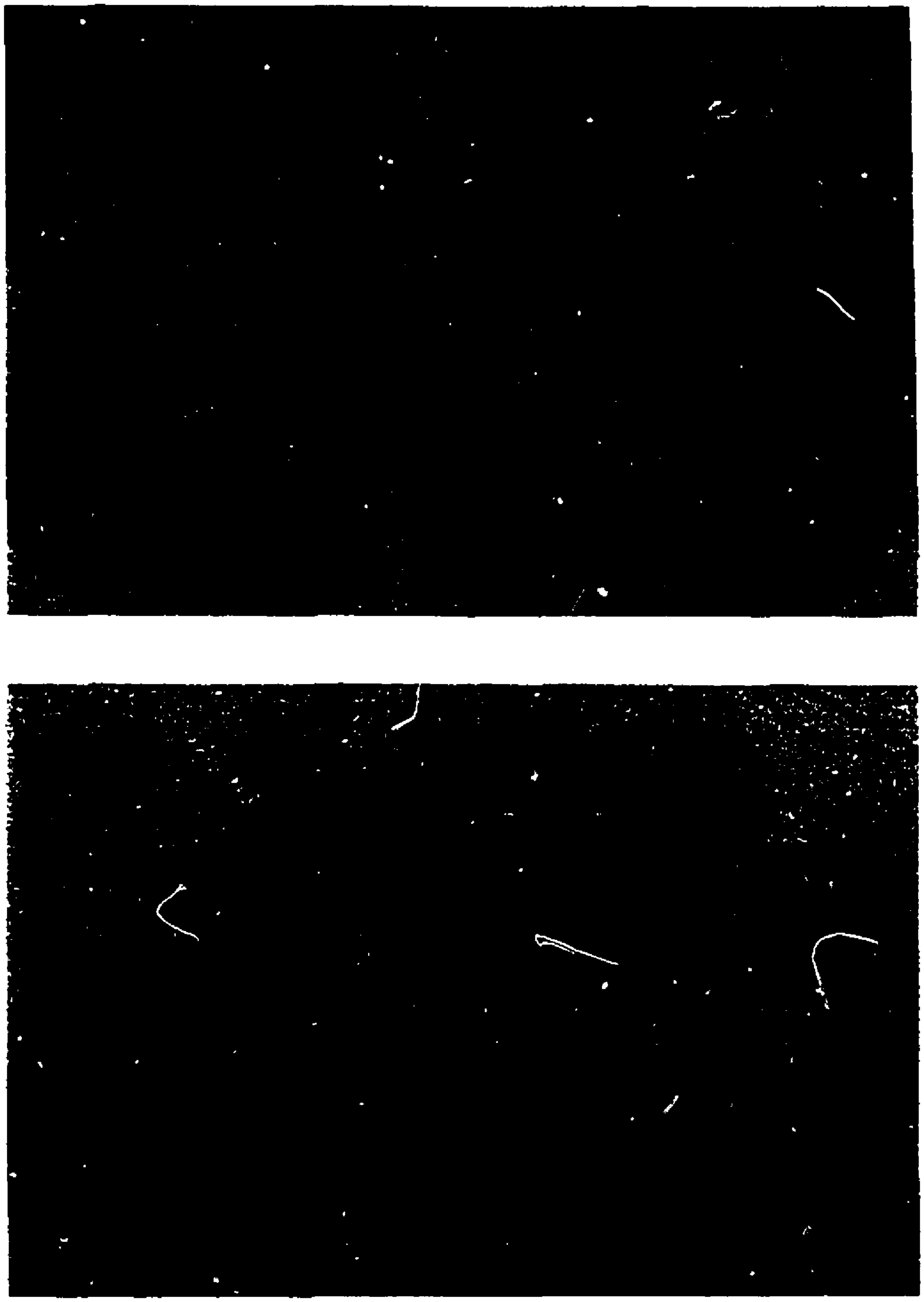

Figure 4.6. Comparison of Heart Sections of ET-A Homozygous (A) and ET-A Wild-type (B) Mice. In ET-A homozygous mice, endocardial cushion defect (arrow) is visible. Heart in ET-A wild-type is normal.

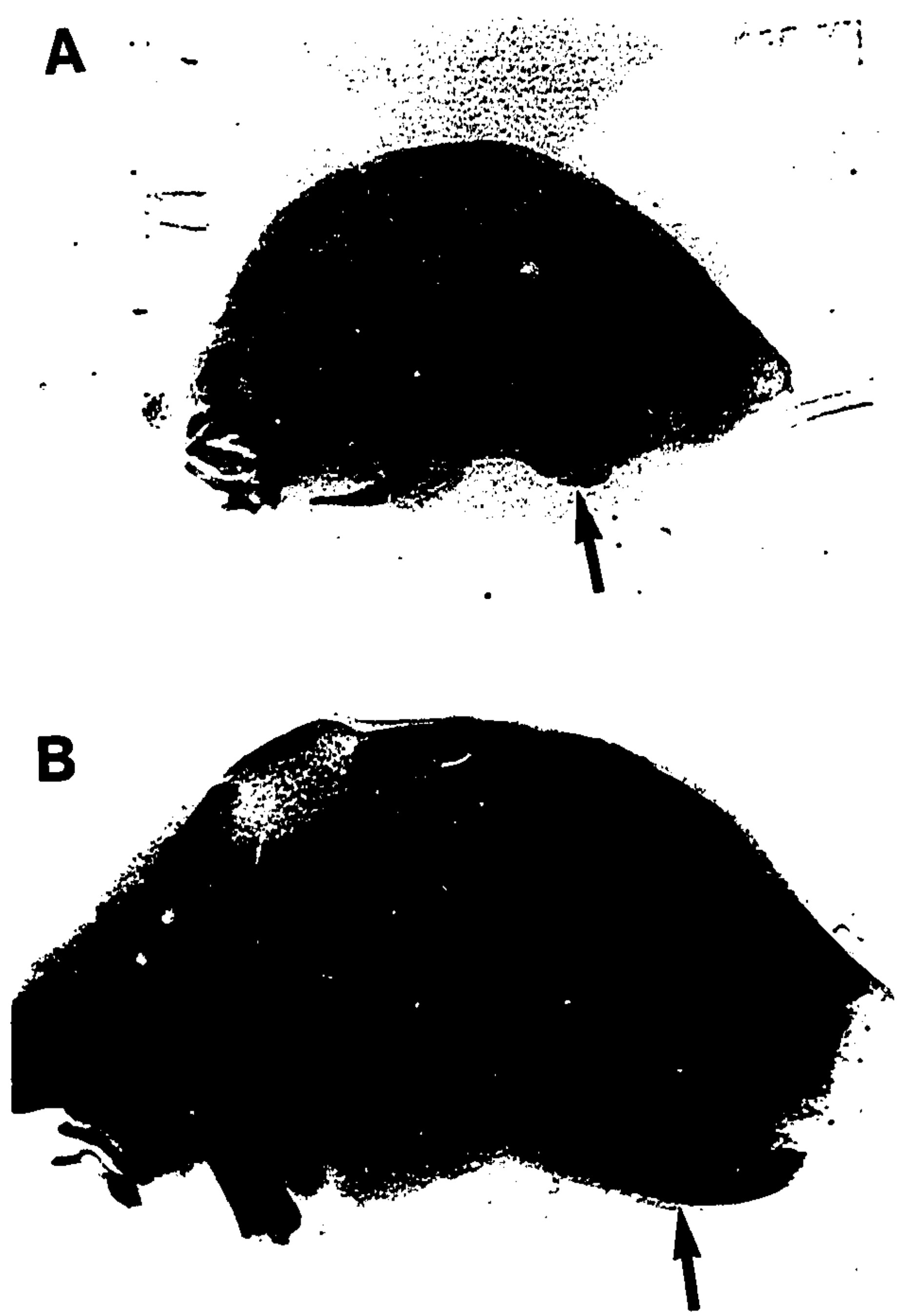

Figure 4. 7. Comparison of Head Skeleton of ET-A Homozygous (A) and ET-A Wild-type (B) Mice. Homozygous mouse has short and deformed mandibular bones (big arrow), absent tympanic ring (small arrow) and auditory ossicle (arrowhead).

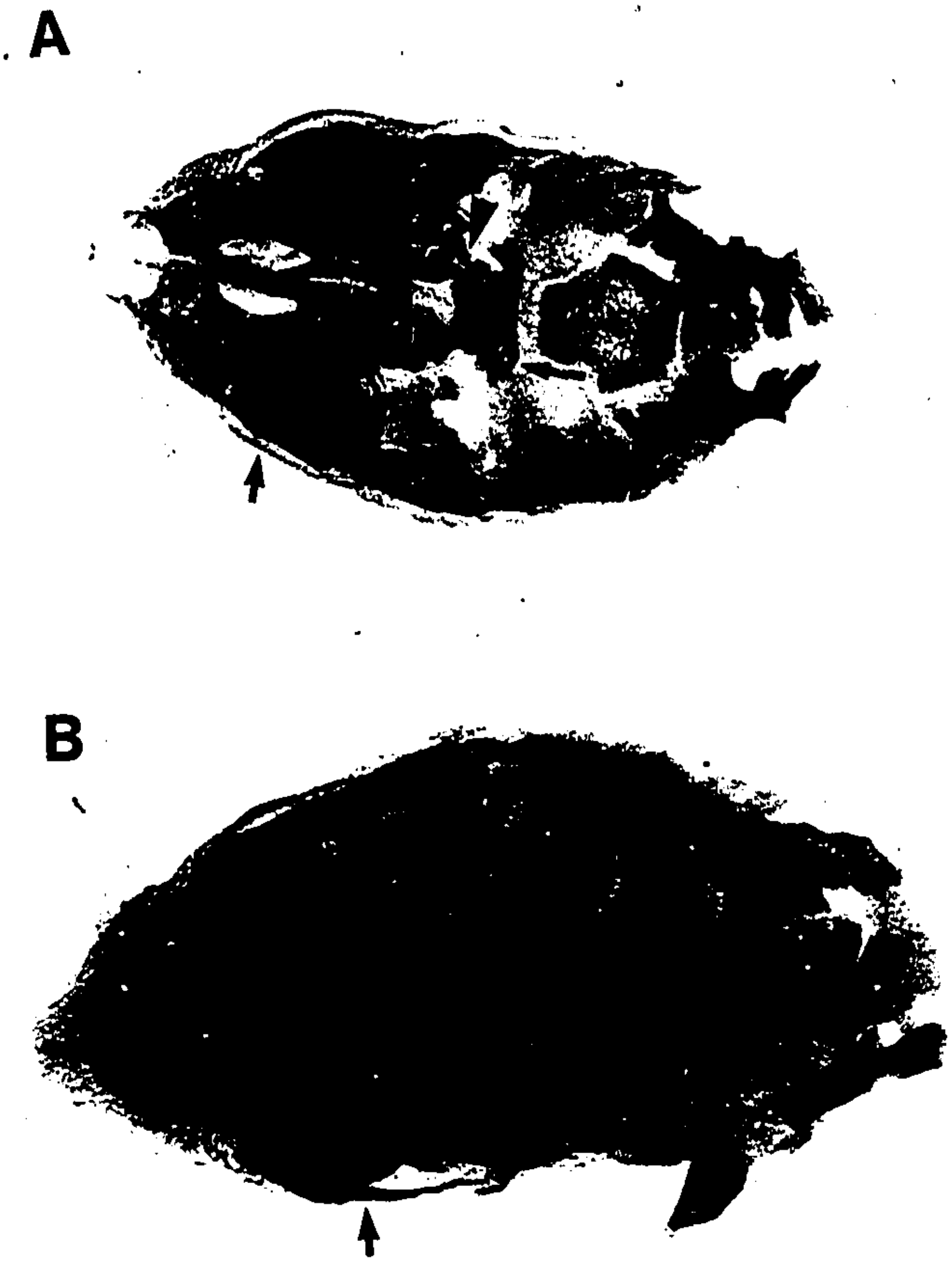

Figure 4.8. Head Skeleton Examination of ET-A Homozygous (A) and ET-A Wild type (B) Mice. Homozygous mouse shows small hyoid bone (big arrow) and aberrant zygomatic bones (small arrow). There are also some abnormal bone structure (arrowhead) in thyrohyoid region of ET-A homozygous mouse.

Figure 4.9. In Situ Hybridization: Expression of ET-A mRNA in the first bronchial arch of ET-A wild-type mouse.

4.4 Discussion

In this study, after disrupting the ET-A gene in mouse ES cells by gene targeting, we stabilished mice bearing the mutant ET-A$^-$ allele. The resulting phenotype shows lethality and malformations of craniofacial tissues in ET-A homozygous, indicating the involvement of ET-A in normal development.

Anoxia due to respiratory failure is major cause of death in ET-A homozygous mice. Rather, some other factors including inability to open the mouth because of poor musculature in the mandibular region and narrowing upper airway may involved in the cause of lethality. Furthermore, ET-A homozygous mice showed difficulty in breathing in response to physical and noxious muscle, indicating the involvement of central respiratory control or respiratory muscle in the cause of lethality. Although the precise mechanism of the lethality is not clear, these results suggest that ET-A may be important in the neural regulation of the respiratory system.

The homozygous ET-A mice show some craniofacial anomalies affecting the mandible, zygomatic and temporal bones, tympanic ring, hyoid, tongue, soft tissue in the anterior neck, palate, outer and middle ears, and endocardial cushion tissue. All of these organs are developed from the pharyngeal arches whose origin is mainly neural crest-derived ectomesenchymal cells. Migration of neural crest cells into the region of pharyngeal arches completes before 10 d.p.c and their differentiation starts thereafter

(Lumsden et al., 1988)). Examination of embryos at serial developmental stages suggests that disturbance in the development of pharyngeal arches already starts around this early stage and their differentiation to Meckel' cartilage, tongue, primordium and other specific tissues are impaired in ET-A homozygous mice.

In this regard, we observed the linkage between the genotype and phenotype are complete in all mice, indicating that these abnormalities can not be due to an incidental mutation. In addition, ET-A has a stimulatory effect on tongue development in organ culture and high ET-A gene expression is detected in the pharyngeal arches at the early stage of embryonic organogenesis by in situ hybridization. These findings indicate the involvement of ET-A in pharyngeal arch development.

Epithelial cells in the pharyngeal arches seems to express ET-A. It is clear that pivotal events in organ development in the pharyngeal region as well as in many other regions include epithelial-mesenchymal interactions. Although the precise mechanism of epithelial-mesenchymal interactions is not clear, several growth factors, for example members of the transforming growth factor-ß family (Curdon, 1992), are considered to be involved in these contractions. Our results strongly suggest that ET-A may affect the epithelial-mesenchymal interactions to induce pharyngeal arch development. Thus the present data indicate a novel physiological role of ET-A in ontogeny in mammals.

Previous studies demonstrated mice mutant for homeotic genes such as Hox-1.5 (Chisaka et al., 1991), or Hox-1.6 (Lufkin et al., 1991: Chisaka et al., 1992), or retionic acid induced embryopathy manifest the same phenotype of ET-A homozygous mice. There is a gross similarity on chromosomal linkage between man and mice, so it is unlikely that mutation of any homeotic gene contributed to the morphological abnormality in ET-A homozygous mice.

The phenotype of ET-A homozygous mice is quite similar to the human congenital disease known as first pharyngeal arch syndrome, such as Pierre-Robin syndrome. First pharyngeal-arch-derived tissues such as mandible, palate and eye show morphological abnormalities in this syndrome, and it is thought to be due to abnormality in the development of a specific neural crest cell lineage. Future studies are necessary to identify the causative gene(s) of this syndrome. ET-A homozygous mice may be a useful tool to investigate the development of the pharyngeal arch and to clarify the phatogenesis of the first pharyngeal arch syndrome.

This part of the project demonstrated that mice deficient for ET-A manifest severe defects in the development of first branchial arch-derived connective tissues, in which cell lineages originating from the cephalic neural crest play major parts. The first and second part of this project (chapter 2 and 3) indicated that the interaction of ET-3 with ET-B is essential for the normal development of two additional neural crest cell lineages, the vagal neural crest-derived enteric neurons and the trunk neural crest-derived epidermal melanocytes. Therefore, the endothelins and their receptors have an important role in mammalian neural crest development.

Chapter 5

Expression of Endothelin-Converting Enzyme-1 in Human Tissues

5.1 Introduction

The three endothelin isopeptides (ET-1, ET-2, and ET-3) are each produced from corresponding ~200-residue prepropolypeptides that are encoded by separate genes (Arinami et al., 1991). Longer intermediates termed big ET-1, 2 and 3 (38-41 amino acids) are first excised from the (pre-) propeptides by proteases that cleave at sites that contain paired basic amino acids (Xu et al., 1994). Big endothelins which are biologically inactive, are then further cleaved at Trp-21 Val-/Il-22 to produce the 21 residue mature peptides. The importance of precise clipping is illustrated by the finding that the vasoconstrictor activity of ET-1 (1-20) and ET-1 (1-22) is three orders of magnitude weaker than authenic ET-1 (1-21) (Kimuro et al., 1989). C-terminal amidation of Trp-21 also causes a marked decrease in the biological activities of the peptide (Inoue et al., 1989).

The putative endopeptidase(s) that catalyzes the specific cleavage at Trp-21 has been termed endothelin-converting enzyme (ECE) (Xu et al., 1994). Two distinct lines of evidence have indicated that ECE is inhibited by the metalloprotease inhibitor phosphoramidon. First, exogenously administered big ET-1 is converted into mature ET-1 both in whole animals and in isolated perfused organs. Phosphoramidon consistently inhibits the conversion in most assay systems (Matsumura et al., 91: Hioki et al., 1991).

Second, cultured endothelial cells secrete mature and big ET-1 in the ratio of 2:1 to 5:1, indicating an efficient (>60%-80%) conversion of the endogenously produced big ET-1. Phosphoramidon added to the medium decreases the production of mature ET-1, causing a concomitant increase in the amount of big ET-1 (Fukuroda et al., 1990).

Production of ET-1 is regulated at the level of mRNA transcription (Rubanyi and polokoff, 1994). In vascular endothelial cells, the peptide is secreted via the constitutive pathway without further regulation at the level of exocytosis.

Accelerated production of ET-1 in damaged vascular endothelial cells is strongly suggested to be involved in the development of various disorders such as acute myocardial infarction (Margulies et al., 1990), acute renal failure (Shibovta et al., 1990), and post hemorrhagic cerebral vasospasm (Arai et al., 1990).

5.2 Methods

5.2.1 Tissue preparation

Human tissues were collected at autopsy (age range 19-45, 3-10 hrs postmortem). For immunohistochemical studies, tissues were fixed in Bouin's solution containing 75% picric acid, 24% formaldehyde, and 1% glacial acetic acid. Tissues were then washed in 30% ethanol and embedded in paraffin. For in situ hybridization, tissues were immersed in a fixative solution of 4% paraformaldehyde in PBS (pH 7.2) for 4 hrs. Tissues were then washed in PBS containing 15% sucrose and 0.01% sodium ozide at 4° C and cut with a cryostat.

5.2.2 Immunohistochemistry

Multiple-step paraffin sections (5 μm) were immunostained with three polyclonal antisera: ECE-1, big ET-1 and ET-1, by the avidin-biotin-peroxidase complex method. Sections were dewaxed in toluene, dehydrated in ethanol, and immersed in a solution of 2% hydrogen peroxide in PBS to inhibit endogenous peroxidase activity. After three 5 mins washes in PBS, sections were incubated with 10% normal goat serum for 1 hr at room temperature. The serum was drained and sections were incubated with primary antisera overnight at 4°C. Sections were washed, incubated with biotinylated goat anti-rabbit IgG antiserum for 45 mins, washed in PBS, and incubated with avidin-biotin peroxidase complex. The immunoreaction sites were visualized in a solution of diaminobenzidine and hydrogen peroxidase. After counterstained with haematoxylin and cleared, sections were mounted in permount. As control, some sections of each organ were incubated with normal goat serum instead of the primary antisera or with the antiserum/antigen mixture. The light-microscopical sections were examined for ECE-1 immunoreactivity (ECE-1-ir), big ET-1-ir, and ET-1-ir.

5.2.3 In Situ Hybridization

In situ hybridization was carried out by a modification of a method reported previously (Giaid et al., 1991). Briefly, the tissues were fixed in paraformaldehyde and cut with a cryostat. ECE-1 probes were then labeled using ^{35}S-UTP.

5.3 RESULTS

Immunohistochemistry confirmed the presence of ECE-1-ir in endothelial cells and some parenchymal cells in a variety of human tissues. The most intense immunoreactivity for ECE-1 was localized primarily to endothelial cells of all kind of vessels in most organs investigated including brain, heart, aorta, lung, liver, pancreas, stomach, duodenum, ileum, colon, adrenal, kidney, testis, ovary, uterus, and vagina. ECE-1-ir was also seen in epithelial cells of respiratory, gastrointestinal, urinary and reproductive systems. Inflammatory cells in the respiratory, gastrointestinal and reproductive tracts showed moderate staining for ECE-1. ECE-1-ir was also seen in cortical neurons (Figure 5.1), and in smooth muscle cells of pulmonary and systemic vessels.

Immunostaining of the heart revealed strong ECE-1-ir over endothelial cells of coronary vessels and endocardium, and moderate staining in the myocardial cells (Figure

5.2 A).In the aorta, diffuse ECE-1-ir was seen in endothelial and smooth muscle cells (Figure 5.2 B).

In the lung, immunoreactivity for ECE-1 was observed in the surface epithelium, endothelial cells, and to a lesser extent in vascular smooth muscle cells. In the airway epithelium, weak to strong diffuse cytoplasmic staining was seen over ciliated and basal cells. Endothelial cells of all kinds of vessels including capillaries, veins and arteries showed moderate staining for ECE-1. Inflammatory cells also showed moderate ECE-1-ir. Big ET-1 showed similar pattern of localization to ECE-1-ir.

In different parts of the gastrointestinal tract, moderate level of ECE-1-ir was detected in epithelial, endothelial, and inflammatory cells. Examination of stomach revealed strong staining in epithelial cells of gastric pits and endothelial cells of blood vessels. Moderate staining was seen in epithelial cells of gastric glands and inflammatory cells. Strong ECE-ir was seen in epithelial cells of villi in duodenum, jejunum, and ileum (Figure 5.3). Moderate staining was also seen in inflammatory cells of these tissues. In the colon, diffuse strong staining was seen in tubular epithelial cells of colonic crypts, inflammatory cells and endothelial cells of blood vessels.

Adrenal glands displayed strong ECE-1-ir in both medulla and cortex. ECE-1-ir was localized to adrenal epithelial cells and endothelial cells of sinoids and blood vessels.

The light microscopical sections of pancreatic tissues revealed strong ECE-1-ir over ductal epithelial cells and islet of Langerhans and moderate ECE-1-ir in acinar cells and vascular endothelial cells (Figure 5.4 A). Big ET-1 was colocalized with ECE-1 in the islet cells but not in the acinar or ductal cells (Figure 5.4 B).

In the liver, weak to moderate staining was seen over endothelial cells of hepatic sinusoids, veins and arteries as well as hepatocytes. Examination of kidney's tissues revealed strong ECE-1-ir in ductal epithelial cells (Figure 5.5 A) and vascular endothelial cells, including those of the glomerulus (Figure 5.5 B).

The light microscopical sections of reproductive organs showed moderate staining in different parts of this system. Sections of ovary revealed diffuse moderate staining in follicular epithelial cells, fibrocytes and endothelial cells. Uterus sections showed moderate ECE-1-ir in myocardial cells and endothelial cells of blood vessels. Examination of vagina sections showed moderate staining in stratified squamous noncornified epithelial cells, endothelial cells of blood vessels, inflammatory cells and sebaceous glands. Testis sections revealed moderate staining in spermatogoniums and spermatocytes, mild staining in leydig cells and interstitial tissues.

The light microscopical examination of skin revealed diffuse moderate ECE-1-ir in stratum granulosum, and endothelial cells of blood vessels.

The distribution of ECE-1 mRNA demonstrated by in-situ hybridization was similar to the distribution of ET-1-ir (Figure 5.6). The most striking expression was seen over the endothelial cells of most of the organs examined. No hybridization signals were seen over control sections.

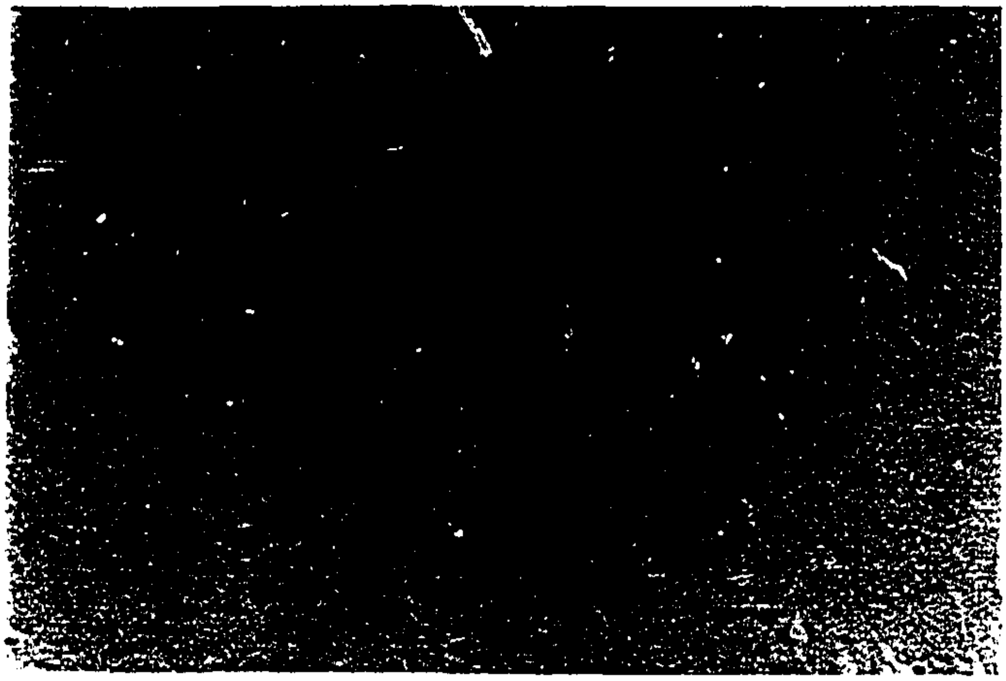

Figure 5.1 ECE-1-ir in human brain section. Arrow indicates a neuron.

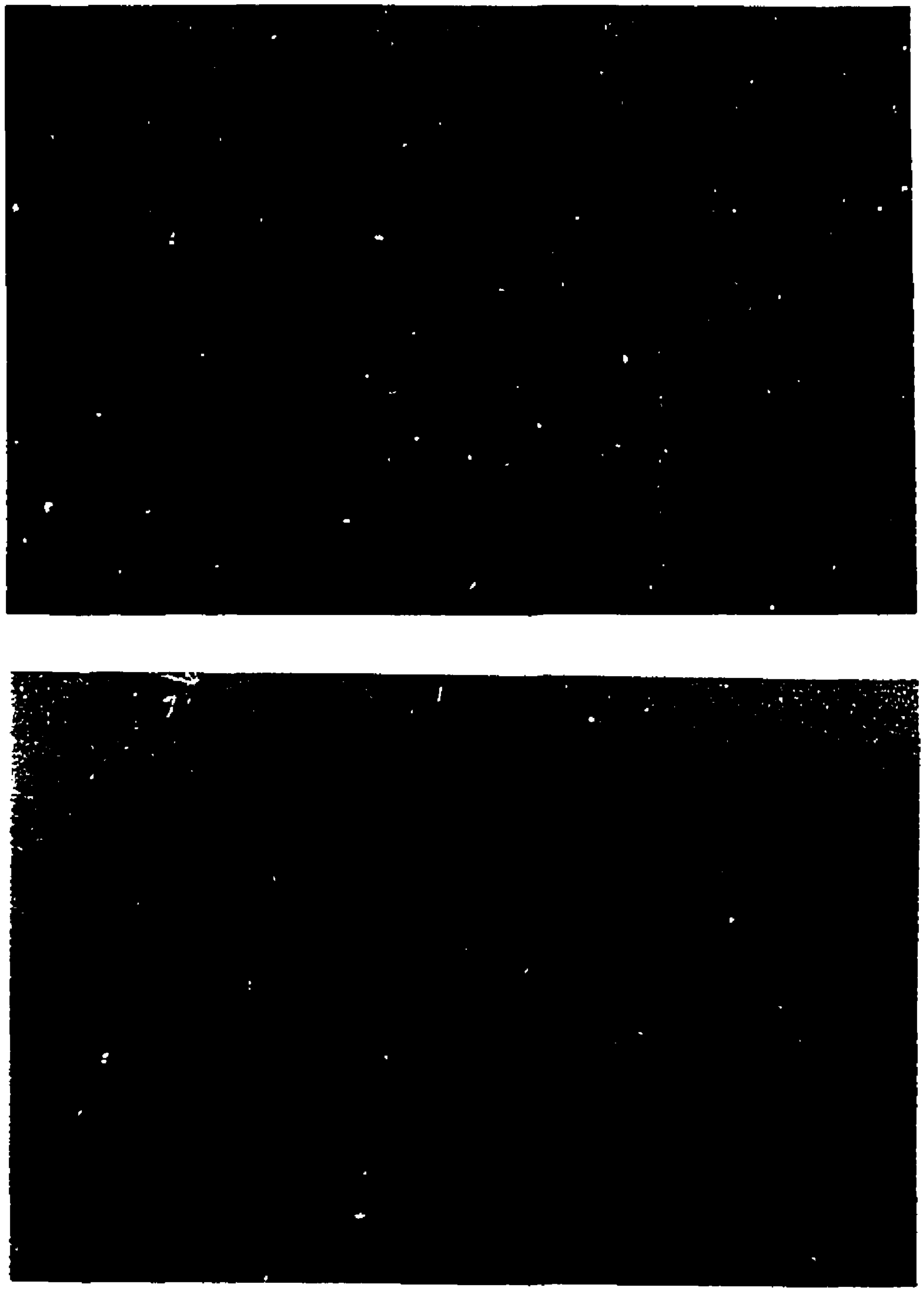

Figure 5.2.

A: ECE-1-ir in Human Heart Section. Small arrow indicates coronary artery and big arrow indicates cardiac myocyte.

B: ECE-1-ir in Human Aorta. Arrowhead indicates endothelial cells.

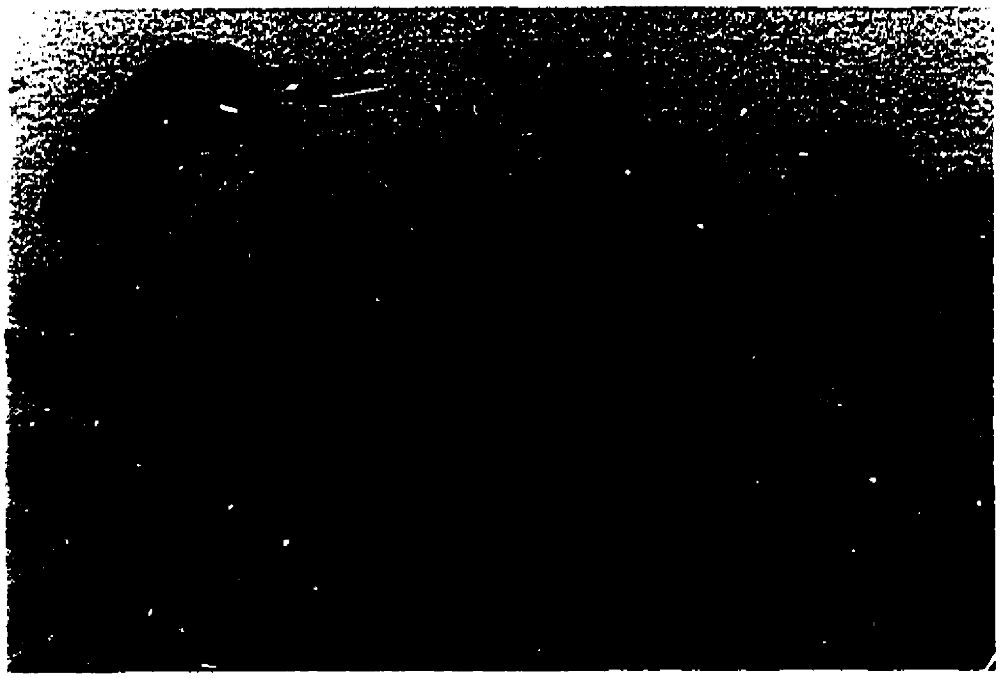

Figure 5. 3.

ECE-1-ir in Human Intestine Section.

Big arrow indicates epithelial cells of villi, and small arrow indicates inflammatory cells.

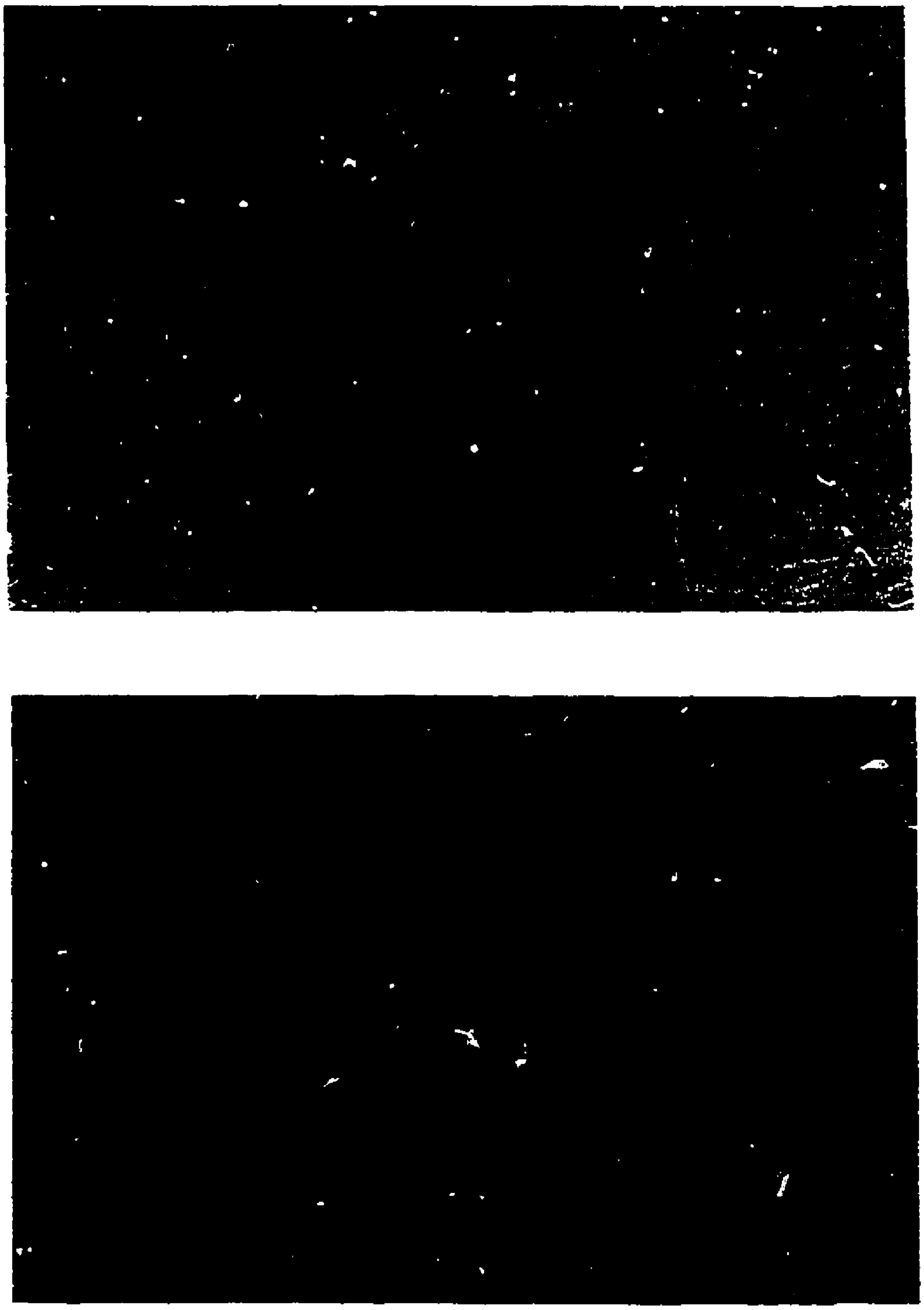

Figure 5.4. A: ECE-1-ir in Human Pancreas Section. B: Big ET-1-ir in human pancreas section. Big arrows indicate ductal epithelial cells, and small arrows indicate islet cells.

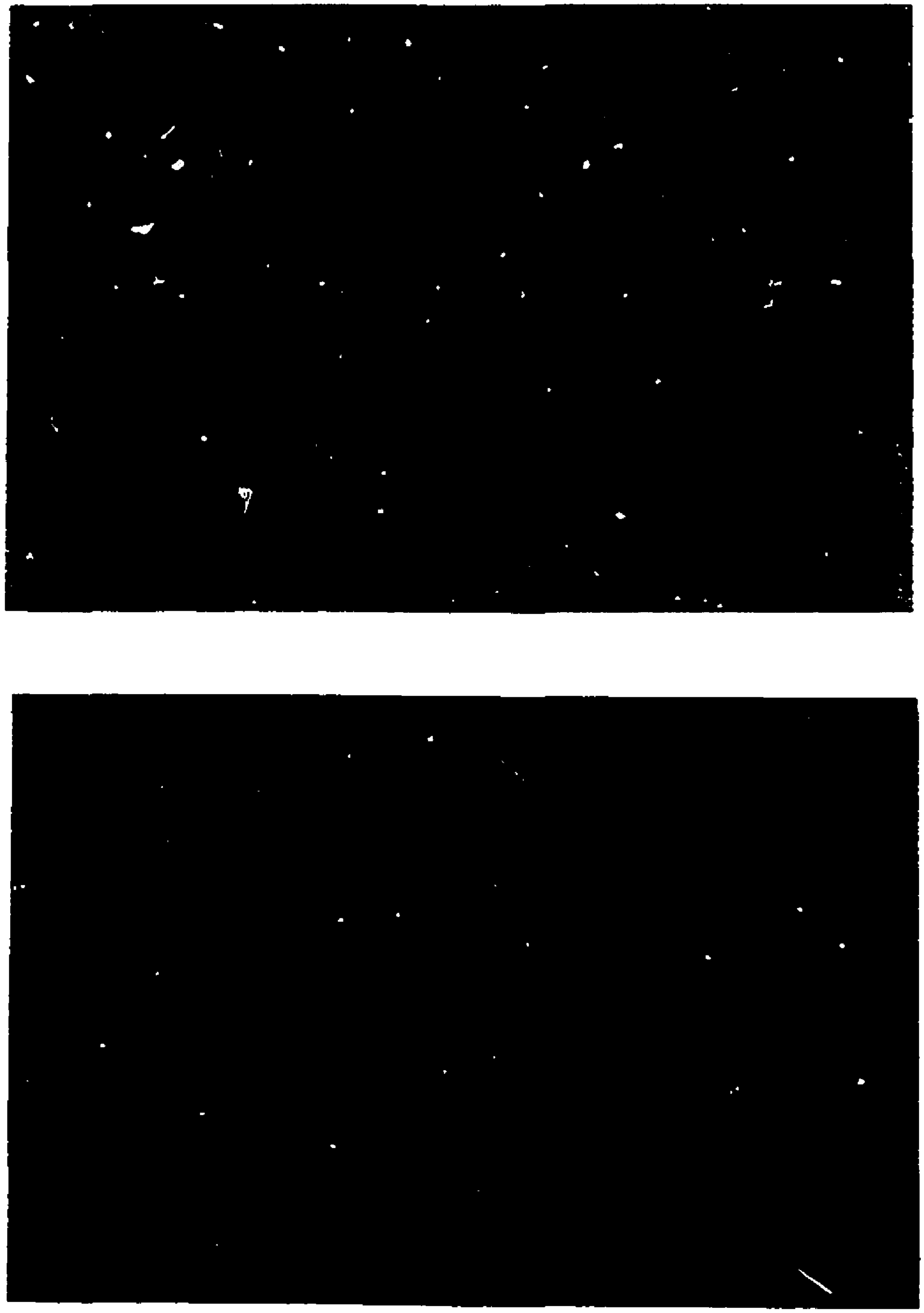

Figure 5.5.

A and B, ECE-1-ir in human kidney section.

Small arrow indicates epithelial cells, and big arrow indicates glomeruli.

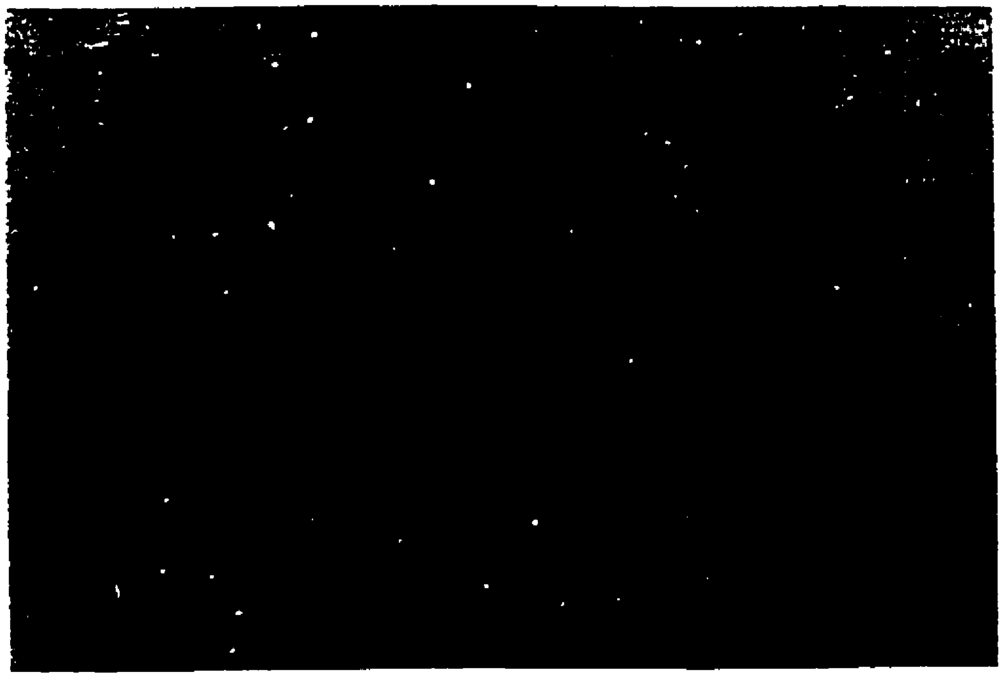

Figure 5.6 Expression of ECE-1 mRNA in human liver section.

5.4 Discussion

Since the initial report of its existence (Yanagisawa et al., 1988), ECE has been considered to be a potential site of regulation of endothelin production as well as a plausible target for therapeutic intervention in the endothelin system. Xu et al. have recently reported the isolation, cloning, and cellular expression of bovine endothelin-converting enzyme-1 (ECE-1) (Xu et al., 1994). In the present study we investigated the expression of human tissues using immunohistochemistry and in situ hybridization, and compared it to those of endothelin-1 and big endothelin-1. Data obtained from this study showed that ECE-1-ir, occur not only in vascular endothelium but also in a number of non vascular cell types in a variety of tissues, including inflammatory cells in the lung, spleen, and colon; epithelial cells of the respiratory, reproductive, gastrointestinal and urinary tract; cortical neurons; smooth muscle cells of pulmonary and systemic vessels, and cardiac myocytes and islet of langerhans. In situ hybridization also confirmed the expression of ECE-1 mRNA in similar sites to those of immunostaining. These findings shows the cellular localization of ECE-1 throughout the human body, and demonstrate that ECE-1 is expressed in similar and different sites to ET-1.

Our immunohistochemical data demonstrated similar colocalization of ECE-1, big ET-1 , and to a lesser degree ET-1 in various human organs. Previous culture experiments provided evidence that a portion of ECE-1 is expressed endogenously and another part is expressed on the cell surface of the transfectants as an ectoenzyme that is capable of cleaving the big ET-1 supplied from outside the cells (Xu et al., 1994). This apparent cell surface conversion of exogenous big ET-1 was much less efficient as compared with the intracellular conversion of endogenous big ET-1. A major finding of this study is similarity in localization of ECE-1-ir and big ET-1-ir in various organs. It seems likely that in these organs ECE-1 functions as a local enzyme, converting big ET-1 to ET-1. However, ECE-1-ir and ET-1-ir were found independently, suggesting that at least some of the high levels of circulating plasma big ET-1 is converted in sites far away from its origin. Indeed, these findings suggest an important role for ECE-1 in a number of pathological conditions associated with high level ET-1.

Beside endothelial cells, ECE-1-ir and its mRNA were also expressed in a heterogenous cell populations in cardiovascular, gastrointestinal, urinary, and reproductive systems. It is interesting that ECE-1 is produced by epithelial and inflammatory cells within these organs. Previous studies have demonstrated the localization of ET-1 mRNA and immunoreactivity in similar structures to those of ECE-1 shown in the present study (Rubanyi and Polokoff, 1994)). As well, alterations in the site and level of ET-1 expression have been reported in a number of diseased conditions (Rubanyi and Polokoff, 1994)). Therefore, our current morphological findings suggest that ECE-1 is widely expressed in human tissues and its level of expression may differ under various pathological states.

One important finding in the current study was the localization of ECE-1 in inflammatory cells throughout the body. ET-1 is known to be a product of mono- and polymorphonuclear cells (Masaki, 1992). Furthermore, a number of studies have shown that inflammatory cells express ability to convert and process big ET-1 (Randall, 1994), consistent with our current findings. ET-1 is thought to play an important role in inflammation, and its has been implicated in a number of inflammatory diseases. Interestingly, we have recently noted increased expression of ECE-1 in patients with chronic rhinitis and in patients with interstitial pneumonitis, suggesting a role for ECE-1 in the pathogenesis of these and other inflammatory conditions.

Chapter 6

Conclusions

In the first part of this study, study of ET-B knockout mice, we did not detect an abnormal phenotype in heterozygous or wild type mice. In the homozygous mice, the skin and coat were completely white in >90% of the body surface area. Microscopic examination of skin sections from the homozygous confirmed an absence of melanin pigment in the coat hair and of melanocytes in the hair bulbs in the regions where the coat was white. Histological examination of colon also revealed the myenteric ganglion neurons were completely absent from the distal, spastic segment of the homozygous ET-B colon. These observations are consistent with the idea that the homozygous ET-B mice have defects in the development of two neural crest-derived cell lineages, namely, enteric ganglion neurons and epidermal melanocytes. Piebald-lethal (s^l) mice exhibited a recessive phenotype identical to that of the ET-B knockout mice. In crossbreeding studies, the two mutations showed no complementation. Southern blotting revealed a deletion encompassing the entire ET-B gene in the s^l chromosome. A milder allele, piebald (s), which produces coat color spotting only, expressed low levels of structurally intact ET-B mRNA and protein. These observations indicate that the extent of white spotting is precisely dependent on the dosage of ET-B expression. In contrast, the megacolon phenotype occurred only in the s^l/s^l and ET-B homozygotes, both of which have zero ET-B expression, but almost never in the s/s^l or s/s mice. This is compatible with the idea that the two neural crest-derived cell lineages required different minimal threshold levels of ET-B expression. Our finding also indicate an essential role for ET-B gene in normal development of two neural crest-derived cell lineages, myenteric ganglion neurons and epidermal melanocytes. The aganglionic megacolon seen in s^l/s^l and homozygous ET-B mice is considered to be pathophysiologically analogous to human Hirschsprung's disease. We concluded that defects in the human ET-B gene cause a hereditary form of Hirschsprung's disease that has been recently mapped to human chromosome 13, in which ET-B is located.

From the first part of this project, we concluded defects in the gene encoding the endothelin-B receptor produce aganglionic megacolon and pigmentary disorders in mice and humans. In the next part of this study we demonstrated that a targeted disruption of the mouse endothelin-3 ligand gene produces a similar recessive phenotype of megacolon and coat color spotting. A natural recessive mutation that results in the same developmental defects in mice, lethal spotting (ls), failed to complement the targeted ET-3 allele. The ls mice carry a point mutation of the ET-3 gene, which replaces the Arg residue at the C-terminus of the inactive intermediate big ET-3 with a Trp residue. This mutation prevents the proteolytic activation of big ET-3 by ECE-1. These findings indicate that interaction of ET-3 with the ET-B receptor is essential in the development of neural crest-derived cell lineages. We postulated that defects in the human ET-3 gene may cause Hirschsprung's disease.

In the third part of this project, we examined the phenotype of ET-A homozygous mice and compared with ET-A heterozygous and wild-type mice. Severe craniofacial malformations in tissues derived from the first branchial arch in ET-A homozygous mice was seen, indicating the importance of ET-A in normal development of neural crest-derived tissues.

Cephalic neural crest, trunk neural crest and vagal neural crest are three distinct parts of neural crest-derived tissues. We concluded that ET-A is essential for normal development of pharyngeal arch ectomesenchymal tissues from the cephalic neural crest. ET-B and ET-3 are essential for normal development of epidermal melanocytes from trunk neural crest and myenteric ganglion neurons from the vagal neural crest.

In the last part of this project, we investigated the expression of ECE-1 in human tissues using immunohistochemistry and in situ hybridization, and compared it to those of endothelin-1 and big ET-1. Strong diffuse immunoreactivity (ir) for ECE-1 was localized primarily to vascular endothelial cells of all organs investigated. ECE-1 was also seen in epithelial cells of the respiratory, gastrointestinal, and urinary tracts. Occasionally, ECE-1-ir was seen in cortical neurons and, in smooth muscle cells of pulmonary and systemic vessels. Inflammatory cells in the lungs, spleen and colon showed strong staining for ECE-1. Islet of langerhans showed moderate staining for ECE-1. The pattern of ECE-1 was parallel to that of endothelin-1 and big endothelin-1. In situ hybridization showed expression of the mRNA in similar sites to those of immunostaining. In conclusion, ECE-1 is widely expressed in human tissues and its level of expression may differ under various pathological states.

Current investigations are focused on the role of ECE-1 in normal development.

References

- **Anderson** D. J. 1994. Stem Cells and transcription Factors in the Development of the Mammalian Neural Crest. *FASEB J.*, **8**: 707-713.

- **Arai**, H., Hori, S., Aramori, I., Ohkubo, H., and Makanishi, S. 1990. Cloning and expression a cDNA encoding an endothelin receptor. Nature, **348**: 730-732.

- **Aria**, H., Nakao, K., Takaya, K., Hosoda, K., Ogawa, Y., Nakanishi, S., and Imura. 1993. The human endothelin-B receptor gene: structural organization and chromosomal assignment. *J. Biol. Chem.* **268**: 3463-3470.

- **Arinami**, T., Ishikawa, M., Inoue, A., Yanagisawa, M., Masaki, T., Yoshida, M., and Homaguchi, H. 1991. Chromosomal assignments of the human endothelin family genes: The endothelin 1 gene (EDN1) to 6p23p24, the endothelin 2 gene (EDN2) to 1p34, and the endothelin 3 gene (EDN3) to 20q13.2q13.3. Am. J. Hum. Genet., **48**: 990-996.

- **Badr**, K. F., Munger, K. A., Sugiura, M., Snajdar, R.M., Schwartzberg, M., and Inagami, t. 1989. High and low affinity binding sites for endothelin on cultured rat glomerular mesangial cells. Biochem. biophys. Res. commun. **161**: 776-781.

◆ **Barr**, P. J. 1991. Mammalian subtilisins: the long-sought dibasic processing endoproteases. *Cell* **66**: 1-3.

◆ **Baydoun**, A. R., Dears, S. H., Cirino, G., and Woodward, B. 1989. Effects of endothelin 1 on the rat isolated heart. J. Cardiovasc. Pharmacol., **13**: S193-S196.

◆ **Bloch**, K., Frederich, S., Lee, M., Eddy, R., Shows, T., and Quertermous, T. Structural organization and chromosomal assignment of the gene encoding endothelin. J. Biol. Chem., **264**: 10851-10857.

◆ **Bolger**, G. T., Liard, F., Krogsrud, R., Thibeault, D., and Jaramillo, J. 1990. Tissue specificity of endothelin binding sites. *J. Cardiovasc. Pharmacol.* **16**: 367-375.

◆ **Borges**, R., Von Grafenstein, H., and Knight, D. E. 1989. Tissue selectivity of endothelin. Eur. J. Pharmacol., **165**: 223-230.

◆ **Botting**, R. M., and Vane, J. R. 1990. Endothelins: potent releasers of prostacyclin and EDRF. Pol. J. Pharmacol. Pharm., **42**: 203-218.

- **Bourne**, A., Barnes, K., Taylor, B. A., Turner, A. J., Kenny, A. J. 1989. Membrane peptidases in the pig choroid plexus and on other cell surfaces in contact with the cerebrospinal fluid. Biochem. J., **250**: 69-80.

- **Bronner-Fraser**, M. 1994. Neural Crest Cells Formation and Migration in the Developing Embryo. *FASEB. J.* **8**: 699-706.

- **Clozel**, M., Fischli, W. 1989. Human cultured endothelial cells do secrete endothelin-1. J. Cadiovasc. Pharmacol., **13**: S229-31.

- **Chisaka**. O., and Capecchi, M. R. 1991. Regionally restricted developmental defects resulting from targeted disruption of the mouse homeobox gene hox-1.5. *Nature*. **350**: 473-479.

- **Chisaka**, o., Music, T. S., and Capecchi, M. R. 1992. Developmental defects of the ear, cranial nerves and hindbrain resulting from targeted disruption of the mouse homeobox gene hox-1.6. *Nature*. **355**: 516-520.

- **Curdon**, J. B. 1992. The generation of discovery and pattern in animal development. *Cell*. **68**: 185-199.

- **Conte**, D., Questino, P., Fillo, S., Nordio, M., Isidori, A., and romanelli, F. 1993. Endothelin stimulates testosterone secretion by rat leydig cells. J, Endocrinol., **136**: R1-R4.

- **D'Orleans-Juste**, P., Lidbury, P. S., Warner, T. D., Vane, J. R. 1990. Intravascular big endothelin increases circulating levels of endothelin-1 and prostanoids in the rabbit. Biochem. Pharmacol., **39**: R21-22.

- **De May**, J. G., and Vanhoutte, P. M. 1982. Heterogenous behavior of the canine arterial and venous wall: Importance of endothelium. *Circ. Res.* **51**: 439-447.

- **De Nucci**, G., Thomas, R., D'Orleans, Juste, P., Antunes, E., Walter, C., Warner, T. D., and Vane, J. r. 1988. Pressor effects of circulating endothelin are limited by its removal in the pulmonary circulation and by the release of prostacyclin and endothelium derived relaxing factor. *Proc. Natl. Acad. Sci. USA.*, **85**: 9797-9800.

- **Eglen**, R. M., Michel, A. D., Sharif, N. A., Swank, S. R., and Whiting, R. L. 1989. The pharmacological properties of the peptide, endothelin. *Br. J. Pharmacol.*, **97**: 1297-1307.

- **Eipper**, B. A., Milgram, S. L., Husten, E. J., Yun, H. Y., and Mains, R. E. 1993. Peptidylglycine alpha-amidating monooxygenase: a multifunctional protein with catalytic, processing, and routing domains. *Prot. Sci.* **2**,: 489-497.

- **Emori**, Y., Hirata, Y., Ohata, K., Shirchiri, M., Marumo, F. 1989. Secretory mechanism of immunoreactive endothelin-1 in cultured bovine endothelial cells. Biochem. *Biophys. Res. Commun.*, **13**: S229-231.

- **Fabbrini**, M., Vitale, A., Pedrazzini, E., Nitti, G., Zamai, M., Tamburin, M., Caiolfa, V., Patrono, C., and Benatti, L. 1993. In vivo expression of mutant preproendothelins: hierarchy of processing events but not strict requirement of Trp-Val at the processing site. *Proc. natl. Acad. Sci. USA*. **90**: 3923-3927.

- **Fisher**, E., and Scambler, P., 1994. Human haploinsufficiency-one for sorrow, two for joy. *Nature Genet*. **7**: 5-7.

- **Fukuroda**, T., Noguchi, K., Tsuchida, S., Nishikibe, M., Ikemoto, F., Okada, K., et al. 1990. Inhibition of biological actions of big endothelin-1 by phosphoramidon. *Biochem. Biophys.Res. Commun.*, **172**: 390-395.

- **Furchgott**, R. F., and Zawadzki, J. V. 1980. The obligatory role of endothelial cells in the relaxation of arterial smooth muscle by acetylcholin. *Nature*, **288**: 373-376, 1980.

- **Giaid**, A., Gibson, S. J., Herrero, M. T., Gentleman, S., Legon, S., Yanagisawa, M., Masaki, T., Ibrahim, N. B. N., Roberts, G. W., Rossi, M. L., and Polak, J. M. 1991. Topographical localization of endothelin mRNA and peptide immunoreactivity in neurons of the human brain. *Histochemistry*, **95**: 303-314.

- **Giaid**, A., Polak, J. M., Gaitonde, V. 1991. Distribution of endothelin-like immunoreactivity and mRNA in the developing and adult human lung. *Am J Respir Cell Mol Biol.* **4**: 50-58.

- **Giaid**, A., Michel, R. P., Stewart, D. J., Sheppard, M., Corrin, B., Hamid, Q. 1993a. Expression of endothelin-1 in lungs of patients with cryptogenic fibrosing alveolitis. *The Lancet*, **341**: 1550-1554.

- **Giaid**, A., Yanagisawa, M., Langleben, D., Michel, R. P., Levy, R., Shennib, H., Kimura, S., Masaki, T., Duguid, W. P., Stewort, D. J. 1993b. Expression of endothelin-1 in the lungs of patients with pulmonary hypertension. *N. Eng J. Med.* **328**: 1732-1739.

- **Gillemot**, F., Johnson, J. E., Auerbach, A., Anderson, D. J., and Joyner, A. L. Mammalian achaete-scute homolog 1 is required for the early development of olfactory and autonomic neurons. *cell* **75**: 463-476.

- **Henry**, P. J., Rigby, P. J., Self, G. J., Preuss, J. M., and Goldie, R. G. 1990. Relationship between endothelin 1 binding site densities and constrictor activities in human animal airway smooth muscle. *Br. J. Pharmacol.*, **100**: 786-792.

- **Hicky**, K., Rubanyi, G., Paul, R., and Highsmith, R. 1985. Characterization of a coronary vasoconstrictor produced by cultured endothelial cells. *Am. J. Physiol.*, **248**: C550-C556.

- **Hioki**, Y., Okada, K., Ito, H., Matsuyama, K., Yano, M. 1991. Endothelin-converting enzyme of bovine carotid artery smooth muscles. *Biochem. biophys. Res. Commun.* **174**: 446-451.

- **Hosoda**, K., Hammer, R. E., Richardson, J. A., Bayanish, A. G., Cheung, J. G., Giaid, A., and Yanagisawa, M. 1994. Targeted and natural (piebald-lethal) mutations of endothelin-B receptor gene produce megacolon associated with spotted coat color in mice. *Cell* **79**:1277-1285.

- **Hosoda**, K., Nakao, K., Tamura, N., Arai, H., Ogawa, Y., Suga, S., Nakanishi, S., and Imura, H. Organization, structure, chromosomal assignment, and expression of the gene encoding the human endothelin A receptor. *J Biol. Chem.* **267**: 18797-18804.

- **Ihara**, M., Noguchi, K., Saeki, T., Fukuroda, T., Kimura, S. 1992. Biological profiles of highly potent novel endothelin antagonists selective for the ET_A receptor. *Life Sci.*, **50**: 247-455.

- **Ikadai**, H., Fujita, H., Agematsu, Y., and Imamichi, T. 1979. Observation of Congenital Aganglionosis Rat (Hirschsprung's Disease Rat) and its Genital Analysis. *Cong. Anom.* **19:** 31-36

- **Ikegawa**, R., Matsumura, Y., Tsukahara, Y., Takaoka, M., Morimoto, S. 1990. Phosphoramidon, a metalloproteinases inhibitor, suppresses the secretion of endothelin from cultured endothelial cells by inhibiting a big endothelin-1 converting enzyme. *Biochem. Biophys. Res. Commun.*, **171**: 669-675.

- **Inagaki**, H., Bishop, A. E., Escring, C., Wharton, J., Allen-Mersh, T. G., and Polak, J. M. 1991. Localization of endothelin like immunoreactivity and endothelin binding sites in human colon. *Gastroenterology* **101**: 47-54.

- **Inoue**, A., Yanagisawa, M., Kimura, S., Goto, K., and Masaki, T. 1989. The human endothelin family: three structurally and pharmacologically distinct isopeptides predicted by three separate genes. *Proc. Natl. acad. sci., USA.*, **86**: 2863-2867.

- **Inoue**, A., Yanagisawa, M., Takuwa, Y., Mitsui, Y., Kobayashi, M., and Masaki, T. 1989. The human preproendothelin 1 gene. Complete nucleotide sequence and regulation of expression. *J. Bio. Chem.*, **264**: 1495-1459.

- **Jackson**, I. J. 1991. Mouse coat color mutations: a molecular genetic receptor which spans the centuries. *Bioassay* **13**: 439-446.

- **Kapur**, R. P., Yost, C., and Palmiter, R. D. 1992. A transgenic model for studying development of the enteric nervous system in normal and aganglionic mice. *Development* **116**: 167-175.

- **Karwatowska Prokopczuk**, E., and Wennmalm, A. 1990. Effects of endothelin on coronary flow, mechanical performance, oxygen uptake, and formation of purines and on outflow of prostacyclin in the isolated rabbit heart. *Circ. Res.*, **66**: 46-54.

- **Kawano**, Y., Yoshida, K., Yoshimi, H., Kuramochi, M., and Omae, T. 1989. The cardiovascular effect of intracerebroventricular endothelin in rats. *J. Hypertens.*, **7**: S22-S23.

- **Kimura**, C., Itoh, Y., Ohkubo, S., Ogi, K., and Fujino, M. 1989. Cloning and sequencing of a canine gene segment mature endothelin. *Nucleic Acids Res.*, **17**: 3290-1989.

- **Komuro**, I., Kurihara, H., Sugiyama, T., Yoshizumi, M., Takaku, F., and Yazaki, Y. 1988. Endothelins stimulates *c fos* and *c myc* expression and proliferation of vascular smooth muscle cells. *FEBS Lett.*, **238**: 249-252.

- **Kosaka**, T., Suzuki, N., Ishibashi, Y., Matsumoto, H., Ohkubo, S., Ogi, K., Kitada, C., Onda, H., and Fujino, M. 1994. Biosynthesis of human endothelins in transformants expressing cDNA for human prepro-endothelins. *J. Biochem. (Tokyo)* **116**:443-449.

♦ **Kozuka**, M., Ito, T., Hirose, S., Takahashi, K., and Hagiwara, H. 1989. Endothelin induces two types of contractions of rat uterus: Phasic contractions by way of voltage dependent calcium channels and developing contractions through a second type of calcium channel. *Biochem. Biophys. Res. Commun.*, **159**: 317-323.

♦ **Kundu**, G. C., Wilson, I. B. 1992. Identification of endothelin-converting enzyme in bovine lung membranes using a new flurogenic substrate. Life Sci., **50**: 965-970.

♦ **Kundu**, G., Wilson, I. B. 1992. Identification of endothelin-converting enzyme in rat lung membranes using a new fluorogenic substrate. *Life Sci.*, **50**: 965-970.

♦ **Kurihara**, Y., Kurihara, H., Suzuki, H., Kodama, T., Maemura, K., Nagai, R., Oda, H., Kuwaki, T., Cao, W., Kamada, N., Jishage, K., Ouchi, Y., Azuma, S., Toyoda, Y., Ishikawa, T., Kumada, M., and Yazaki, Y. 1994. Elevated blood pressure and craniofacial abnormalities in mice deficient in endothelin-1. *Nature* **368**: 703-710.

- **Lamont**, M. A., Fitchett, M., and Dennis, N. R. 1989. Interstitial deletion of distal 13q associated with Hirschsprung'disease. *J. Med. Genet.* **26**: 100-104.

- **Lane**, P. W. 1966. Association of Megacolon with two recessive Spotting Genes in the Mouse. *J. Hered.* **57**: 29-31.

- **Lehoux**, S., Plante, G. E., Sirois, M. G.., Sirois, P., D'Orleans-Juste, P. 1992. Phosphoramidon blocks Big endothelin-1 but not endothelin-1 enhancement of vascular permeability in the rat. *Br. J. Pharmacol.*, **107**: 996-1000.

- **Liang**, J. C., Juarez, C. P., and Goldberg, M. F. 1994. Bilateral bicolored irides with Hirschsprung' disease. *Archr Ophtalmol.* **101**: 63-74.

- **Lufkin**, t., Dieruch, A., Lemaur, M., Mark, M., and Chambon, P. 1991. Disruption of the Hox-1.6 Homeobox gene results in defects in a region corresponding to its rostral domain of expression. *cell*, **66:** 1105-1119.

- **Lyon**, M. F. and Searle, A. G. 1989. Genetics Variants and Strains of the Laboratory Mouse (Oxford, Englnd: Oxford University Press). Mayer, T. C., 1989. Enhancement of Melanocyte Development from Piebald Neural Crest by a Favorable Tissue Environment. *Dev. Biol.* **56**: 255-262.

- **Makino**, S., Hashimoto, K., Hirasawa, R., Hattori, T., Kageyama, J., and Ota, Z. 1990. Central interaction between endothelin and brain natriuretic peptide on pressor and hormonal responses. *Brain Res.*, **534**: 117-121.

◆ **Margulies**, K. B., Hildebrand, F. L., Lerman, A., Perrella, M. A., Burnett, J. C. 1990. Increased endothelin in experimental heart failure. *Circulation*, **82**: 2226-2230.

◆ **Masaki**, T., Yanagisawa, M., and Goto, K. 1992. Physiology and pharmacology of endothelins. *Med. Res. Rev.*, **12**: 391-421.

◆ **Matsumoto**, H., Suzuki, N., Onda, H., and Fujino, M. 1989. Abundance of endothelin-3 in rat intestine, pituitary gland and brain. *Biochem. Biophys. Res. Commun.* **164**: 74-80.

◆ **Matsumura**, K., Abe, I., Tsuchibashi. T., Tominaga, M., Kobayashi, K., and Fujishima, M. 1991. Central effect of endothelin on neurohormonal responses in conscious rabbits. *Hypertension*, **17**: 1192-1196.

◆ **Matsumura**, Y., Ikegawa, R., Tsukahara, Y., Morimoto, S. 1991. Conversion of big endothelin-1 by two types of metalloproteinases of cultured porcine vascular smooth muscle cells. *Biochem. Biophys. Res. Commun.*, **178**: 890-905.

◆ **Mayer**, T. C. 1977. Enhancement of melanocyte development from piebald neural crest by a favorable tissue environment. *Dev. Biol.* **56**: 255-262.

◆ **Mc Cabe**, L., Grifin, L. D., Kinzer, A., Chandler, M., Beckwith, J. B., and Mccabe, E. R. B. 1990. Overo Lethal White Foal Syndrome: Equine Model of Aganglionic Megacolon (Hirschsprung Disease). *Am. J. Med. Genet.* **36:** 336-340.

- **Mc Mahon**, E. G., Fok, K. F., Moore, W. M., Smith, C. E. 1990. In vitro and in vivo activity of chymotrypsin-activated big endothelin. *Biochem Biophys Res Commun.*, **166**: 436-442.

- **Mc Mahon**, E. G., Palomo, M., Moore, W. M., McDonald, J. F., Stern, M. K. 1991. Phosphoramidon blocks the pressor activity of porcine big endothelin-1 in vivo and conversion of big endothelin-1 to endothelin-1. *Proc. Natl. Acad. Sci. USA*, **88**: 703-707.

- **Metallinos**, D. L., Oppenheimer, A. J., Rinchink, E. M., Russell, L. B., Dietrich, W., and Tilghman, S. M. 1994. Fine structure mapping and deletion analysis of the murine piebald locus. *Genetics*. **136**:217-223.

- **Miyauchi**, T., Yanagisawa, M., Tomizawa, T., Sugishita, Y., Suzuki, N., Fujino, M., Ajisaka, R., Goto, K., and masaki, T. 1989. Increased plasma concentrations of endothelin 1 and big endothelin 1 in acute myocardial infarction. *Lancet* **2**: 53-56.

- **Moncada** S, Gryglewski R, Bunting S, and Vane G R. 1976. An enzyme isolated from arteries transforms prostaglandin endoperoxidaes to an unstable substance that inhibits platelet aggregation. *Nature*, **263**:663-665.

◆ **Muldoon**, L. L., Roland, K. D., Forsythe, M. I., and Macun, B. E. 1989. Stimulation of phosphatidylinositol hydrolysis, diacylglycerol release, and gene expression in response to endothelin, a potent new agonist for fibroblasts and smooth muscle cells. *J. Biol. Chem.*, **246**: 8529-8536.

◆ **Naruse**, K., Naruse, M., Watanabe, Y., Yoshihara, I. 1991. Molecular form of immuno reactive endothelin in plasma and urine of normal subjects and patients with various disease states. *J. Cardiovasc. Phamacol.*, **17**: S506-508.

◆ **Ninomiya**, H., Uchida, Y., Saotome, M., Nomura, A., Ohse, H., Matsumoto, H., Hirata, F., and Hasegawa, S. 1992. Endothelins constrict guinea pig tracheas by multiple mechanisms. *J. Pharmacol. Exp. Ther.*, **262**: 570-576.

◆ **Ohlstein**, E. H., Nambi, P., Douglas, S. A., Edwards, R. M., Gelliai, M., Lago, A., Leber, J. D., Cousins, R. D., Gao, A., Frazee, J. S., Peishoff, C. E., Bean, J. W., Eggleston, D. S., Elshourbagy, N. A., Kumar, C., Lee, J. A., Brooks, D. P., Weinstock, J., Feuerstein, G., Ruffolo, R. R., Gleason, J. G., and Ellimot, J. D. 1994. SB 209670, a rationally designed potent nonpeptide endothelin receptor antagonist. *Proc. Natl. Acad. Sci. USA.* **91**: 8052-8056.

◆ **Okata**, K., Arai, Y., Hata, M., Matsuyama, K., and Yano, M. 1993. Big endothelin-1 structure important for specific processing by endothelin-converting enzyme of bovine endothelial cells. *Eur. J. Biochem.* **218**: 493-498.

◆ **Pachnis**, V., Mankoo, B., and Costantini, F. 1993. Expression of the c-ret proto-oncogene during mouse embryogenesis. *Development* **119**: 1005-1017.

◆ **Parker-Botelho**, L. H., Cade, C., Phillips, P. E., and Rubanyi, G. M. 1992. Tissue specificity of endothelin synthesis and binding. In endothelin, edited by G. M. Rubanyi, *Oxford University Press. New York.* pp.72-102.

◆ **Pavan**, W. J., and Tilghman, S. M. 1994. Piebald lethal (s^1) acts early to disrupt the development of neural crest-derived melanocytes. *Proc. Natl. Acad. Sci. USA.* **91**: 7159-7163.

◆ **Puffenberger**, E. G., Hosoda, K., Washington, S. S., Nakao, K., deWit, D., Yanagisawa, M., and Chakaravarti, A. 1994. A missense mutation of the endothelin-B receptor gene in multigenic Hirschsprung' disease. *Cell* **79**: 1265-1270.

◆ **Puffenberger**, E. G., Kauffman, E. R., Bolk, S., Matise, T. C., Washington, S. S., Angrist, M., Weissenbach, J., Graver, K. L., Mascari, M., Lada, R., Slaugenhoupt, S. A., and Chakravarti, A. 1994. Identity by descent and association mapping of a recessive gene for Hirschsprung disease on human chromosome 13q22. *Hum. Mol Genet.* **3**: 1217-1225.

- **Randall**, M. D. 1994. Endothelins: from laboratory to clinic? *Lancet*, **344**: 832-833.

- **Romeo**, G., Ronchetto, P., Luo, Y., Barone, V., Seri, M., Ceccherini, I., Pasini, B., Bocciardi, R., Lerone, M., Kaariainen, H., and Martucciello, G. 1994. Point mutations affecting the tyrosine kinase domain of the RET proto-oncogene in Hirschsprung's disease. *Nature* **367**: 377-380.

- **Rothman**, T. P., Goldowitz, D., and Gersshon, M. D. 1993. Inhibition of migration of neural crest-derived cells by the abnormal mesenchyme of the presumptive aganglionic bowel of ls/ls mice: analysis with aggregation and interspecies chimeras. *Dev. Biol.* **159**: 559-573.

- **Rubanyi**, G. M., and Polokoff, M. A. 1994. Endothelins: molecular biology, biochemistry, pharmacology, physiology, and pathophysiology. *Pharmacol. Rev.*, **46**:325-415.

- **Sakamoto**, A., Yanagisawa, M., Sawamura, T., Enoki, T., Ohtani, T., Sakurai, T., Nakao, K., Toyo-oka, T., and Masaki, T. 1993. Distinct subdomains of human endothelin receptors determine their selectivity to ET_A-selective antagonist and ET_B-selective agonists. *J. Biol. Chem.* **268**: 8547-8553.

- **Sakuria**, T., Yanagisawa, M., Takuwa, Y., Miyazaki, H., Kimura, S. 1990. Cloning of a cDNA encoding a non-isopeptide selective subtype of the endothelin receptor. *Nature,* **348**:732-735.

- **Sawamura**, T., Kimura, S., Shinmi, O., Sugita, Y., Kobayashi, M., Mitsui, Y., et al. 1990. Characterization of endothelin converting enzyme activities in soluble fraction of bovine cultured endothelial cells. *Biochem. Biophys. Res. Commun.* **163**: 1138-1144.

- **Schini**, V. B., Vanhoutte, P., M. 1991. ET-1: a potent vasoactive peptide. *Pharmacol Toxical.*, **69**:303-309.

- **Schuchardt**, A., D'Agati, V. Larson-Blomberg, L., Costonini, F., and Pachnis, V., Defects in the Kidney and Enteric Nervous System of Mice Lacking the Tyrosine Kinase Receptor. *Ret. Nature.* **367**: 380-383.

- **Shah**, K. N., Dalal, S. J., Desai, M. P., Sheth, P. N., Joshi, N. C., and Ambani, L. M. 1981. White forelock, pigmentary disorder of irides, and long segment Hirschsprung disease: possible variant of Waardenburg syndrome. *J. Pediatr.* **99**: 432-435.

- **Shibouta**, Y., Suzuki, N., Shiko, A., Matsumoto, H., Terashita, Z., Kondo, K. 1990. Pathophysiological role of endothelin in acute renal failure. *Life Sci.*, **46**: 1611-1118.

- **Silvers**, W. K. 1979. The coat colors of mice: A model for mammalian gene action and interaction *(New York: Springer-Verlag, Inc.)*.

- **Simonson**, M. S., and Dunn, M. J. 1990. Cellular signaling by peptides of the endothelin gene family. *FASEB J.*, **4**: 2989-3000.

- **Simonson**, M. S., and Herman, W. H. 1993. Protein kinase C and protein tyrosine kinase activity contribute to mitogenic signaling by endothelin-1: cross-talk between G protein-coupled receptors and pp60$^{c\text{-}src}$. *J. Biol. Chem.* **268**: 9347-9357.

- **Simonson**, M. S., Wann, S., Mene, P., Dubyak, G. R., Kester, M., and Dunn, M. J. 1989. Endothelin-1 activates the phosphoinositide cascade in cultured glomerular mesangial cells. *J. Cardiovasc. Pharmacol.*, **13**: S80-S83.

- **Steiner**, D. F., Smeekens, P., Ohagi, S., and Chan, S. J. 1992. The new enzymology of precursor processing endoproteases. *J. Biol. Chem.* **267**: 23435-23438.

- **Suzuki**, E., Hirata, T., Matsuoka, H., Sugimoto, T., Hayakawa, H., Shin, W. S., Toyoaka, T., and Sugimoto, T. 1991. Effects of artrial natriuretic peptide on endothelin induced vasoconstriction and intracellular calcium mobilization. *J. hypertens.* **9** : 927-934

♦ **Suzuki,** N., Matsumoto, H., Miyauchi, T., Got, K., Masaki, T., Tsuda, M., and Fujino, M. 1990. Endothelin-3 concentrations in human plasma: The increased concentrations in patients undergoing haemodialysis. *Biochem. Biophys. Res. Commun.* **169**: 809-815.

♦ **Svane**, D., Larsson, B., Alm, P., Andersson, K. E., and Forman, A. 1993. Endothelin 1: immunocytochemistry, localization of binding sites, and contractile effects in human uteroplacental smooth muscle. *Am. J. Obstet. Gynecol.* **168**: 233-241.

♦ **Takuwa**, n., Takwa, Y., Yanagisawa, M., Yamashita, K., and Masaki, T. 1989. A novel vasoactive peptide endothelin stimulates mitogenesis through inositol lipid turnover in Swiss 3T3 fibroblasts. *J.Bio. Chem.*, **249**:7856-7861.

♦ **Tsuchiya**, K., Naruse, M., Sanaka, T., Naruse, K., Nitta, K., Demura, H., and Sugino, N. 1989. Effects of endothelin on renal regional blood flow in dogs. *Eur. J. Pharmacol.* **166**: 541-543.

♦ **Warner**, T. D., Mitchell, J. A., D'orleans-Juste, P., Ishii, K., Forstermann, U., Murad, F. 1992. Characterization.of endothelin-converting enzyme from endothelial cells and rat brain: detection of the formation of biologically active ET-1 by rapid bioassay. *Mol. Pharmacol.*, **41**: 399-403.

- **Watanabe**, H., Miyazaki, H., Kondoh, M., Masuda, Y., Kimura, S., Yanagisawa, M., Masaki, T., and Murakami, K. 1989. Two distinct types of endothelin receptors are present on chick cardiac membranes. *Biochem. Biophys. Res. Commun.*, **161**: 1252-1259.

- **Webster**, W. 1992. Embryogenesis of the enteric ganglia in normal mice and in mice that develop congenital aganglionic megacolon. *J. Embryol. Exp. Morphr* **30**: 573-585.

- **Xu**, D., Emoto, N., Giaid, A., Slaughter, C., Kaw, S., deWit, D., and Yanagisawa, M. 1994. ECE-1: a membrane-bound metalloprotease that catalyzes the proteolytic activation of big endothelin-1. *cell* **78**: 473-485.

- **Yada**, Y., Higuchi, K., and Imokawa, G. 1991. Effects of endothelins on signal transduction and proliferation in human melanocytes. *J. Biol. Chem.* **266**: 18352-18357.

- **Yamaji**, T., Johshita, H., Ishibashi, M., Takaku, F., Ohno, H. 1990. Endothelin family in human plasma and cerebrospinal fluid. *J. Clin. Endo. Met.*, **71**: 1611-1615.

- **Yanagisawa**, M. 1994. The endothelin system: a new target for therapeutic intervention. *Circulation*, **89**: 1320-1322.

- **Yanagisawa**, M., Kurihara, H., Kimura, S., Tomobe, Y., Kobayashi, M., and Masaki, T. 1988. A novel potent vasoconstrictor peptide produced by vascular endothelial cells. *Nature*, **332**: 411-415.

- **Yang**, D., and Clark, K. E. 1992. Effects of endothelin 1 on the uterine vasculature of the pregnant and estrogen treated nonpregnant sheep. *Am. J. Obstet. Gynecol.*, **167**: 1642-1650.

- **Yohn**, J. J., Smith, C., Stevens, T., Hoffman, T. A., Morelli, J. G., Hurt, D. L., Yanagisawa, M., Kane, M. A., and Zamora, M. R. 1994. Human melanoma cells express functional endothelin-1 receptors. *Biochem. Biophys. Res. Commun* **201**: 449-457.

- **Yoshizumi**, M., Kurihara, H., Sagiyama, T., Takaku, F., Yanagisawa, M., Maskki, T.1989. Hemodynamic shear stress stimulates endothelin production by cultured endothelial cells. *Biochem. Biophys. Res. Commun.*, **161**: 859-867.

- **Zachary**, I., and Rozengurt, E. 1992. Focal adhesion kinase ($p125^{FAK}$): a point of convergence in the action of neuropeptides, integrins, and oncogenes. *Cell*, **71**: 891-894.